THE
PHYSICAL REVIEW

A journal of experimental and theoretical physics established by E. L. Nichols in 1893

SECOND SERIES, VOL. 79, NO. 4 AUGUST 15, 1950

Fine Structure of the Hydrogen Atom.* Part I

WILLIS E. LAMB, JR., AND ROBERT C. RETHERFORD†
Columbia Radiation Laboratory, Columbia University, New York, New York
(Received April 10, 1950)

The fine structure of the hydrogen atom is studied by a microwave method. A beam of atoms in the metastable $2^2S_{1/2}$ state is produced by bombarding atomic hydrogen. The metastable atoms are detected when they fall on a metal surface and eject electrons. If the metastable atoms are subjected to radiofrequency power of the proper frequency, they undergo transitions to the nonmetastable states $2^2P_{1/2}$ and $2^2P_{3/2}$ and decay to the ground state $1^2S_{1/2}$ in which they are not detected. In this way it is determined that contrary to the predictions of the Dirac theory, the $2^2S_{1/2}$ state does not have the same energy as the $2^2P_{1/2}$ state, but lies higher by an amount corresponding to a frequency of about 1000 Mc/sec. Within the accuracy of the measurements, the separation of the $2^2P_{1/2}$ and $2^2P_{3/2}$ levels is in agreement with the Dirac theory. No differences in either level shift or doublet separation were observed between hydrogen and deuterium. These results were obtained with the first working apparatus. Much more accurate measurements will be reported in subsequent papers as well as a detailed comparison with the quantum electrodynamic explanation of the level shift by Bethe.

Among the topics discussed in connection with this work are (1) spectroscopic observations of the H_α line, (2) early attempts to use microwaves to study the hydrogen fine structure, (3) existence of metastable hydrogen atoms, their properties and methods for their production and detection, (4) estimates of yield and r-f power requirements, (5) Zeeman and hyperfine structure effects, (6) quenching of metastable hydrogen atoms by electric and motional electric fields, (7) production of a polarized beam of metastable hydrogen atoms.

A. INTRODUCTION

IN August, 1947 a brief account[1] was given of the use of microwaves to solve the problem of the fine structure of atomic hydrogen. A deviation from the predictions of the Dirac theory amounting to about 1000 Mc/sec. in the position of the $2^2S_{1/2}$ level was definitely established. The accuracy of these first measurements amounted to perhaps 100 Mc/sec. It was planned at that time to follow quickly with a paper setting forth fully the method and theory of the experiment. The first apparatus was necessarily crude, and we were already working on a new and improved version. Our goal was first set to achieve an accuracy of 10 Mc/sec., but this has since been changed to 1 Mc./sec. The program was a large one and encountered unexpected difficulties which required much time to surmount. As a result, the paper promised two years ago was delayed.

We are at present engaged in making the final measurements on our new apparatus. Owing to the increased experimental accuracy, a large number of small experimental and theoretical effects must be taken into account in the analysis of the data. It is felt that if all of these matters were also incorporated into one paper, the result would be unwieldy, and not do justice to the simple basic ideas involved in the experiment.

Therefore, it is planned to write a series of papers, of which this is the first. This article will contain a brief history of the problem, an account of the considerations involved in the choice of method, estimates of effects to be expected, a description of the apparatus constructed prior to May, 1947, and the experimental results obtained with that apparatus. Since the numerical estimates of expected effects depend considerably on quantities which were unknown when such estimates were first made, it has been decided to make use of present knowledge where convenient in order to avoid lengthy discussions. As a result, some of the estimates are applicable to later forms of the apparatus, but it is thought that this will not cause undue confusion to the reader.

The theory of the hydrogen atom and the Zeeman effect of its fine structure and hyperfine structure has

* Work supported jointly by the Signal Corps and ONR.
† Submitted by Robert C. Retherford in partial fulfillment of the requirements for the degree of Doctor of Philosophy in the Faculty of Pure Science, Columbia University.
[1] W. E. Lamb, Jr. and R. C. Retherford, Phys. Rev. **72**, 241 (1947). A later value for the term shift of 1062±5 Mc/sec. was reported by R. C. Retherford and W. E. Lamb, Jr., Phys. Rev. **75**, 1325 (1949).

been reviewed, since it is necessary for an understanding of the experimental results. In the present paper, we have taken into account effects of the order of 10 Mc/sec. or larger, leaving a more accurate description to a later paper where it is really needed. The effect of reduced mass has been largely ignored, and only slight attention given to the existence of the anomalous magnetic moment of the electron.

B. DISCUSSION OF THE PROBLEM

1. General Considerations

The hydrogen atom is the simplest one in nature, and the only one for which essentially exact calculations can be made on the basis of theory. The theoretical discussions now usually start with the Dirac equation for the motion of an electron in the pure Coulomb field of a fixed point charge. Corrections for the motion of the proton, its possible finite size, and the hyperfine structure due to its magnetic moment can be taken into account to a good approximation. The same is true of the effects due to interaction of the electron with the quantized electromagnetic field which were discovered by Bethe[2] subsequent to the establishment of departures from the Dirac theory.

According to the Bohr[3] theory of 1913, the energy levels of a hydrogen-like atom are given by the equation

$$W_n = -hcRZ^2/n^2, \tag{1}$$

where R is the Rydberg wave number, $h=2\pi\hbar$ is Planck's constant, and c is the velocity of light. For an infinitely heavy nucleus, $R=(109{,}737.3)$ cm^{-1}. The transition from state $n=3$ to $n=2$ gives the red H_α line. This was discovered by Michelson and Morley[4] in 1887 to be actually a doublet. An explanation of this fine structure was given by Sommerfeld[3] in 1916 in terms of the relativistic variation of electron mass with velocity. The two possible motions for principal quantum number $n=2$ differed in energy by

$$\Delta W_2 = (\alpha^2/16)hcR[1+0(\alpha^2)], \tag{2}$$

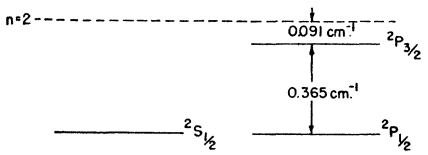

FIG. 1. Fine structure of $n=2$ levels of hydrogen according to the Dirac theory.

with $\alpha=1/(137.030)$ the fine structure constant (Birge, 1941).

When quantum mechanics was first introduced, it was found that, although the Bohr formula could be derived, the approximate inclusion of relativistic effects gave a separation of 8/3 times that of Eq. (2), which was at least in rough agreement with the observations of the time. Only when the Goudsmit-Uhlenbeck and Thomas model[3] of a spinning electron was incorporated into the theory did it again become possible to derive Eq. (2). Instead of two levels, there were now three, as shown in Fig. 1. This theory indicated that there should be an exact coincidence of the $2^2S_{1/2}$ and $2^2P_{1/2}$ levels, but the calculation was not entirely free of ambiguity, since the ratio 0/0 appeared in the derivation.

The Dirac theory of the electron of 1928 automatically endowed the electron with relativistic properties, spin and magnetic moment, and predicted the fine structure pattern of Fig. 1 without the above-mentioned ambiguity. The energy levels of a hydrogen-like atom are given by

$$W = mc^2\{[1+(\alpha Z)^2(n-|K| + (K^2-\alpha^2Z^2)^{\frac{1}{2}})^{-2}]^{-\frac{1}{2}}-1\}, \tag{3}$$

where $|K|=j+\frac{1}{2}$. In agreement with Fig. 1, the levels having the same principal quantum number n and inner quantum number j are degenerate. Expansion of Eq. (3) in powers of αZ gives

$$W_{nj} = -Z^2hcR/n^2 - (\alpha^2Z^4hcR/n^3)[(j+\tfrac{1}{2})^{-1}-(3/4n)]+\cdots. \tag{4}$$

According to this, the doublet separation for the $n=2$ state of hydrogen is

$$\Delta W_2 = (\alpha^2/16)hcR, \tag{5}$$

agreeing with the Sommerfeld result, since the next term in the expansion is entirely negligible for present purposes.

Although the treatment of the hydrogen atom given by the Dirac theory was beautiful and satisfying, the theory carried with it some strange consequences arising from the existence of the negative energy states. It was therefore considered highly desirable to subject the fine structure predictions to careful experimental tests. These were at first, naturally enough, observations on the spectrum of the hydrogen atom. Any departure from theory would be ascribed to one or more of the following causes: (1) error in the Dirac equation, (2) modification of the Coulomb law of attraction between electron and proton, possibly by a short-range non-electromagnetic interaction,[5] or positron theoretic vacuum polarization[6] effects, (3) some

[2] H. A. Bethe, Phys. Rev. **72**, 339 (1947). Relativistic calculations of the term shift have been made by N. M. Kroll and W. E. Lamb, Jr., Phys. Rev. **75**, 388 (1949) and J. B. French and V. F. Weisskopf, Phys. Rev. **75**, 1240 (1949). Different results have been obtained by A. D. Galinin, J. Exp. Theor. Phys. **19**, 521 (1949); Y. Nambu, Prog. Theor. Phys. **4**, 82 (1949); O. Hara and T. Tokano, Prog. Theor. Phys. **4**, 103 (1949); Fukuda, Miyamoto, and Tomonaga, Prog. Theor. Phys. **4**, 121 (1949).

[3] For a general discussion, see H. E. White, *Introduction to Atomic Spectra* (McGraw-Hill Book Company, Inc., New York, 1934).

[4] A. A. Michelson and E. W. Morley, Phil. Mag. **24**, 46 (1887).

[5] E. C. Kemble and R. D. Present, Phys. Rev. **44**, 1031 (1933); J. M. Jauch, Helv. Phys. Acta. **13**, 451 (1940); A. Sommerfeld, Naturwiss. **29**, 286 (1941), Zeits. f. Physik **118**, 295 (1941); P. Caldirola, Nuovo Cimento **5**, 207 (1948); E. David, Zeits. f. Physik **125**, 274 (1949).

[6] E. A. Uehling, Phys. Rev. **48**, 55 (1935).

finite and physically real remnant of the infinite radiative shift in the frequencies of all spectral lines predicted by the 1930 calculations of Oppenheimer,[7] or (4) unexplained effects. The work of Bechert and Meixner[8] showed that hyperfine structure and reduced mass effects could not be responsible for appreciable discrepancies.

2. Spectroscopic Observations of the H_α Line

The history of the spectroscopic work on the H_α doublet is a long one, starting with the first resolution of the doublet structure in 1887 and continuing today. The reader is referred to the 1938 paper by Williams[9] for an account of the earlier work. By 1940 the situation had become very unclear. On the one hand, the work of Houston[10] and Williams[9] indicated rather probable discrepancies between theory and experiment Pasternack[11] had shown that these could be explained if the $2^2S_{1/2}$ level were raised relative to the $2^2P_{1/2}$ level by about 0.03 cm^{-1}. In 1940 Drinkwater, Richardson, and Williams,[12] on the other hand, attributed any discrepancies to impurities in the source.

The theorists who attempted to account for Pasternack's shift in terms of a departure from the Coulomb law[5] were frustrated by the smallness of their predictions, or misled[13] by inadequacies in their theories. They rather eagerly hailed the results of Drinkwater, Richardson, and Williams[12] which confirmed the Dirac theory.

Postwar measurements by Giulotto[14] pointed again to a discrepancy, and recently Kuhn and Series,[15] using a liquid hydrogen cooled discharged tube, reported a shift of $2^2S_{1/2}$ of 0.043 ± 0.006 cm^{-1}.

The H_α complex of lines has two main peaks separated by about 0.317 cm^{-1}, and in the work of Williams with deuterium the lines had Doppler widths of 0.120 cm^{-1}. Under these circumstances, a really precise spectroscopic check of the theory is exceedingly difficult. It is made even more so by the fact that the intensities of the components often depart from the theoretically predicted values and vary with the discharge conditions.

Only the use of an atomic beam source to reduce the Doppler effect would seem to offer much hope for a real resolution of the H_α complex. The radiative width of the sharpest line would be only about 0.001 cm^{-1} (30 Mc/sec.), but according to estimates made by Mack,[16] the attainable width would be about ten times larger.

3. Possible Use of Radio Waves in Hydrogen Spectroscopy

It was pointed out as early as 1928 by Grotrian[16a] that the selection rules permitted optical transitions with zero change of the principal quantum number, n, and that it should be possible with radio waves to induce such transitions among the states $n=2$ corresponding to the doublet separation $\Delta\tilde{\nu}=0.365$ cm^{-1} or a wave-length $\lambda=2.74$ cm and frequency 10,950 Mc/sec.

There are some German papers[17,18] between 1932 and 1935 dealing with attempts to detect such a transition. At that time, only spark gap oscillators of exceedingly low power output were available for such wave-lengths. One had to work with a continuous spectrum of radiation, using the interference methods to select a reasonably monochromatic range of wave-lengths. The radiation was passed through an absorption vessel containing a hydrogen discharge of the Wood's[19] type, and the attentuation was determined as a function of wave-length. The first worker, Betz, claimed to have observed an absorption in the expected wave-length range of 3 cm. He also obtained selective absorptions at 9 and 27 cm corresponding to transitions between the fine structure states of the levels with $n=3$. Three years later, working in the same laboratory, Haase repeated the experiment more carefully and failed to find any absorption at 9 and 27 cm. He did not study the 3-cm region. Haase made estimates of the selective energy absorption to be expected from excited hydrogen atoms and concluded that it was too small to detect. This question will be discussed in Appendix I from a slightly more modern point of view. Strangely enough, Haase gave no specific reason for the positive results obtained by Betz.

4. Choice of Method

After reading of the Betz-Haase work, we inquired whether microwave techniques, which advanced so much during the war, would now permit a successful and clear-cut determination of the hydrogen fine structure by absorption of the appropriate radiation in a Wood's discharge. In the course of such considerations

[7] J. R. Oppenheimer, Phys. Rev. **35**, 461 (1930).
[8] K. Bechert and J. Meixner, Ann. d. Physik **22**, 525 (1935); G. Breit and G. E. Brown, Phys. Rev. **74**, 1278 (1948).
[9] R. C. Williams, Phys. Rev. **54**, 558 (1938), also F. K. Richtmeyer, *Introduction to Modern Physics* (McGraw-Hill Book Company, Inc., New York, 1934), second edition, p. 398.
[10] W. V. Houston, Phys. Rev. **51**, 446 (1937).
[11] S. Pasternack, Phys. Rev. **54**, 1113 (1938).
[12] Drinkwater, Richardson, and Williams, Proc. Roy. Soc. **A174**, 164 (1940).
[13] Fröhlich, Heitler and Kahn, Proc. Roy. Soc. **A171**, 269 (1939); Phys. Rev. **56**, 961 (1939); B. Kahn, Physica **8**, 58 (1941). See also the objections by W. E. Lamb, Jr., Phys. Rev. **56**, 384 (1939); **57**, 458 (1940) supported by calculations of J. M. Blatt, Phys. Rev. **67**, 205 (1945); and by M. Slotnick and W. Heitler, Phys. Rev. **75**, 1645 (1949).
[14] L. Giulotto, Ricerca Scient. **17**, Nos. 2-3 (1947); Phys. Rev. **71**, 562 (1947).
[15] H. Kuhn and G. W. Series, Nature **162**, 373 (1948). These workers have recently communicated an improved value of 0.0369 ±0.0016 cm^{-1}. Proc. Roy. Soc. **A202**, 127 (1950).
[16] J. E. Mack and E. C. Barkofsky, Rev. Mod. Phys. **14**, 82 (1942).
[16a] W. Grotrian, *Graphische Darstellung der Spektren von Atomen* (Verlag Julius Springer, Berlin, 1928).
[17] O. Betz, Ann. d. Physik **15**, 321 (1932).
[18] T. Haase, Ann. d. Physik **23**, 675 (1935).
[19] R. W. Wood, Phil. Mag. **42**, 729 (1921).

FIG. 2. Schematic block diagram of apparatus.

we came upon the idea of a different method, which was actually used. While we did not reach a definite conclusion on the possibility of the use of a Wood's tube method, the indication was rather discouraging. An account of these deliberations, revised in the light of present knowledge, is given in Appendix I. In view of the extreme crudeness of our numerical estimates, it is by no means certain that one could not now detect transitions between the $n=2$ states of atomic hydrogen if the discharge conditions were properly chosen. From consideration of the perturbing effects of electric fields and ion collisions on the energy levels of the atom, however, it seems that even if the transitions could be detected, the results would be of greater value for an indication of the conditions within a Wood's discharge tube than for a determination of fundamental properties of an isolated hydrogen atom.

There are two main methods in radiofrequency spectroscopy. In one, some matter absorbs or otherwise affects the radiation passing through it. In the other, the radiation causes observable changes to take place in the matter. The former method is used in the conventional form of microwave spectroscopy[20] in which the radiation is transmitted through a long path of absorbing gas. The latter method is used in the molecular beam radiofrequency resonance[21] method when the particles absorbing radiation are deflected out of the beam by an inhomogeneous magnetic field. Since the first method did not seem to be too promising for the study of the hydrogen fine structure, we turned to an examination of the possibilities in the second method.

5. Atomic Beam Method

In the case of atomic hydrogen, the $2P$ states decay to the $1S$ state with the emission of a photon of wavelength 1216A in 1.595×10^{-9} sec., and the atom could move only about 1.3×10^{-3} cm in that time, assuming a speed of 8×10^{5} cm/sec. On the other hand, the possibility exists that the $2^2S_{1/2}$ state would be sufficiently metastable so that a beam of particles in this state could be used. If a transition were then induced by radiofrequency or otherwise to a $2P$ state, a decay to $1^2S_{1/2}$ would take place so quickly that the number of excited atoms in the beam would be reduced. If one could then find a detector which responded selectively to the excited hydrogen atoms, one would have the possibility of measuring the energy difference between the metastable $2^2S_{1/2}$ state and the various $2P$ states. The proposed experiment might then be represented in the block diagram in Fig. 2.

For this program to be carried out it was necessary to solve the following problems: (1) production of beam of atoms in the $2^2S_{1/2}$ state and (2) detection of such atoms. The program clearly depended on a knowledge of the properties of metastable hydrogen atoms. Such atoms had never been isolated in any clear-cut experiments, although they had been the subject of much speculation. The next section is devoted to the properties of metastable hydrogen atoms.

6. Metastable Hydrogen Atoms

In 1924, Compton and Russell[22] in trying to explain the large intensity of stellar Balmer lines pointed out that the lower of the two $n=2$ states obtained on the basis of Sommerfeld's theory should be metastable. In 1926, after the spinning electron theory was introduced, Sommerfeld and Unsöld[23] stated that the $2^2S_{1/2}$ state should still be metastable. On the other hand, Franck and Jordan[24] gave reasons for doubting that the $2^2S_{1/2}$ level would be metastable.

A certain amount of experimental work by Snoek, von Keussler and others[25] was carried out to test the Sommerfeld-Unsöld ideas on this point. They studied the relative intensities of the two main groups of components of the H_α line in absorption. If the $2^2S_{1/2}$ state in the absorbing discharge were appreciably metastable, the intensity ratio of the two peaks would be affected. From their results they concluded that the $2^2S_{1/2}$ level was not appreciably metastable.

Rojansky and Van Vleck[26] pointed out that the effect of an external electric field, however small, would mix the degenerate states $2^2S_{1/2}$ and $2^2P_{1/2}$ giving stationary state wave functions

$$\psi=2^{-\frac{1}{2}}[\psi(2^2S_{1/2})\pm\psi(2^2P_{1/2})], \qquad (6)$$

both of which would decay at the rate $(2\tau_p)^{-1}$, so that there could be no metastability. This conclusion, although correct in a sense, is not applicable to the experimentally realized situations where no stationary state exists. This was pointed out by Bethe[25] who gave a systematic theory of the effect of an electric field on the fine structure of hydrogen. In the complete absence of a perturbing electric field, an atom in the $2^2S_{1/2}$ state should have a very long life. (Bethe estimated that the life of an isolated atom would then be several months if relativistic effects were taken into

[20] W. Gordy, Rev. Mod. Phys. **20**, 668 (1948).
[21] J. M. B. Kellogg and S. Millman, Rev. Mod. Phys. **18**, 323 (1946).
[22] K. T. Compton and H. N. Russell, Nature **114**, 86 (1924).
[23] A. Sommerfeld and A. Unsöld, Zeits. f. Physik **36**, 259 (1926); **38**, 237 (1926).
[24] J. Franck and P. Jordan *Anregung von Quantensprüngen durch Stöese* (Verlag Julius Springer, Berlin, 1926), p. 117. W. de Groot and F. M. Penning, *Handbuch der Physik* (1933), second edition, Vol. 23/1, p. 78.
[25] H. A. Bethe *Handbuch der Physik* (1933), second edition, Vol. 24/1, pp. 452–462.
[26] V. Rojansky and J. H. Van Vleck, Phys. Rev. **32**, 327 (1928); V. Rojansky, Phys. Rev. **33**, 1 (1929).

account.) In the presence of a large perturbing electric field, the result would be that of Rojansky and Van Vleck. As the electric field is increased from zero, the lifetime would undergo a change from one limiting value to the other. Bethe showed that the results of von Keussler and Snoek were understandable in terms of the excitation cross sections of the various levels and the quenching of the metastability by the perturbing electric fields of the discharge. For an effective electric field of 10 volts/cm, he found that the life of the $2^2S_{1/2}$ state would be about five times the life τ_p. Over a large range of fields, the life varies inversely as the square of the field strength. Under typical Wood's tube conditions, Bethe estimated that the life would be about $2\tau_p$.

In 1940, Breit and Teller[27] refined some of Bethe's calculations, and discussed the metastability in connection with possible astrophysical applications. They showed that the decay mechanism of double quantum emission to the ground state was more important than the relativistic effects, and that the life of an isolated metastable atom on this basis would be $\frac{1}{7}$ sec.

It was clear to us from the foregoing that the $2^2S_{1/2}$ state would be markedly metastable only if the perturbing fields could be sufficiently reduced. For a beam length of 6 cm and a speed of 8×10^5 cm/sec., a life of the order 0.75×10^{-5} sec. would be necessary for 37 percent of the atoms to survive. According to Bethe's calculations, this would require a perturbing field of $\frac{1}{3}$ volt/cm or less. It would not be easy to keep the electrons and ions formed in the excitation process away from the detector with such fields unless an extremely long beam were used.

In actuality, of course, we now know that the $2^2S_{1/2}$ and $2^2P_{1/2}$ levels are not degenerate. This adds considerably to the stability of $2^2S_{1/2}$ against Stark effect quenching. According to a simple extension of Bethe's calculation given in Appendix II, the lifetime of $2^2S_{1/2}$ in moderate electric fields becomes

$$\tau_s=\tau_p\{\hbar^2(\omega^2+\tfrac{1}{4}\gamma^2)/V^2\}, \qquad (7)$$

where V is the matrix element of the perturbing electric energy and $\hbar\omega$ is the separation of the interacting levels $2^2S_{1/2}$ and $2^2P_{1/2}$. (Breit and Teller have discussed the stabilizing effect of the hyperfine structure splitting and found an increase in τ_s by a factor of four. Since the actual value of $\hbar\omega$ is much larger than the hyperfine structure splitting, the stability will not be much affected by the hyperfine structure, and we shall neglect it here.) According to Eq. (7), for $\omega/2\pi=1000$ Mc/sec., the life τ_s would be about 400 times longer than if there were no removal of the degeneracy.[28]

[27] G. Breit and E. Teller, Astrophys. J. **91**, 215 (1940). A correspondence theoretic analysis of double quantum emission has been given by J. A. Wheeler, J. Opt. Soc. Am. **37**, 813 (1947).

[28] This suggests the need for a reinterpretation of the experiments of Snoek, von Keussler and others. Some of the features which need consideration are indicated in Appendix I.

At the time, however, we did not take the possibility of a natural removal of the degeneracy by such a large amount very seriously, and planned to increase the stability of $2^2S_{1/2}$ by the application of a magnetic field to give a large Zeeman splitting of the states.

The presence of a magnetic field at right angles to the atomic beam would also serve to keep charged particles away from the detector. A third, and really the most important function of the magnetic field will be discussed in Section 14.

7. Production of a Beam of Metastable Hydrogen Atoms

A number of possible methods for the production of a beam of hydrogen atoms in the metastable $2^2S_{1/2}$ state were considered. The simplest source would be a hydrogen discharge tube with a small opening into a vacuum for the emergence of a beam. In the discharge, one would have a mixture of molecular and atomic hydrogen, electrons and ions, and a small proportion of excited atoms, together with a high intensity of Lyman and Balmer radiation. The population of $2^2S_{1/2}$ is estimated in Appendix I to be about 5×10^{10} atoms/cm^3. The question would be whether any appreciable number of these could escape through the hole before being quenched by the Holzmark fields due to ions and electrons simultaneously escaping. Even with the stabilizing effect of a magnetic field, this did not seem to be likely. It would also be possible for some of the normal atoms to be excited optically to the $3P$ level after leaving the discharge, and of these 12 percent[29] would decay to $2^2S_{1/2}$. The numerical estimate of the yield for this was discouraging. Furthermore, there would be a very high background intensity of ultraviolet radiation at the

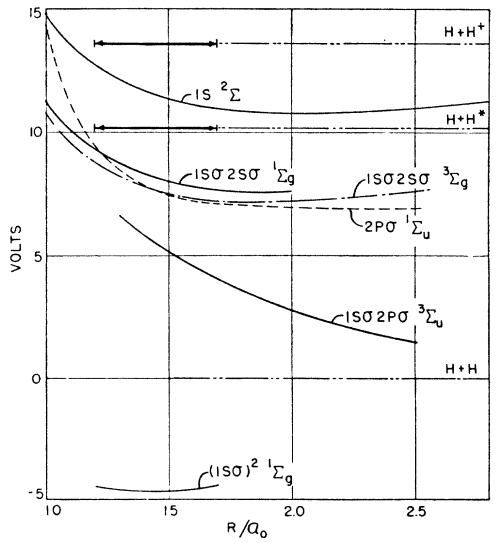

FIG. 3. Electronic energy levels of the hydrogen molecule as a function of internuclear distance.

[29] See reference 25, p. 444.

detector. This could cause trouble since most of the possible detectors of metastable atoms are also photosensitive. Subsequent to the success of the experiment by another method such a Wood's tube source was tried, but did not give positive results.

The second method which we considered was the bombardment of molecular hydrogen with electrons in a field-free region. A possible process is

$$H_2+e\rightarrow H+H^*+e', \tag{8}$$

where H* represents a metastable atom. The potential energy curves for the various excited electronic states of H_2 shown in Fig. 3 are based on calculations by Hylleraas, and by James, Coolidge, and Present.[30] The small segment of the ground state $^1\Sigma_g$ shown represents the limits of zero-point vibration in the lowest vibrational state. According to the Franck-Condon principle, electron bombardment should most strongly excite the $^3\Sigma_g$-state at energies below its dissociation limit into H+H*. One would, however, expect a small yield of metastable atoms for electrons of about 15 ev. Such a "violation" of the Franck-Condon principle would be analagous to the dissociation with ionization,

$$H_2+e\rightarrow H+H^++e'+e'', \tag{9}$$

observed by Bleakney[31] at 18 volts. Besides the $^3\Sigma_g$-curve shown, there are repulsive states leading to H+H*, and hence fast metastable atoms should be produced at higher bombarding energies.

One difficulty with this method of production is that the atomic fragments H+H* move off in directions oriented at random with respect to the electron beam, and hence the detector can conveniently intercept only a small fraction of them. The background effects due to the ultraviolet photons which are produced in molecular hydrogen beginning at 11.5 volts are likely to be troublesome.

In the first form of the apparatus described below, an unsuccessful search was made for metastable hydrogen atoms produced by the bombardment of molecular hydrogen. We now know[32] that had conditions been slightly different, this method would have succeeded.

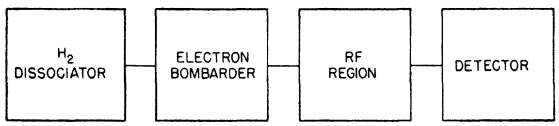

FIG. 4. Modified schematic block diagram of apparatus.

The third method, which was finally adopted, required the separate production of a beam of atomic hydrogen atoms in the ground state and the subsequent bombardment of the beam by electrons with an energy somewhat over the threshold of 10.2 volts for excitation to $2^2S_{1/2}$. The proposed experiment might now be represented by the block diagram shown in Fig. 4.

8. Dissociation of Molecular Hydrogen

A number of methods are available for the production of a beam of atomic hydrogen atoms: (1) Wood's tube, (2) microwave discharge, (3) thermal dissociation in a tungsten furnace. No very compelling reason can be given for the adoption of the last method. We were aware of the work in 1923 of Olmstead and Compton[33] who measured the critical potentials of atomic hydrogen formed in a tungsten oven, and we were greatly assisted by the advice of Dr. O. S. Duffendack[34] who pioneered in research with such ovens. On the other hand, the hydrogen atomic beam work[21] done before the war at Columbia made very successful use of a Wood's tube source. It was felt, however, that the ultraviolet background radiation would be troublesome in our case. The microwave discharge method[35] was ruled out because the leakage of a small amount of r-f power would complicate the spectroscopic observations.

Assuming thermal equilibrium, the extent of the dissociation of molecular hydrogen

$$H_2\rightarrow 2H \tag{10}$$

is given by

$$[P(H)]^2/P(H_2)=K(T), \tag{11}$$

where the equilibrium constant $K(T)$ is given in atmospheres as a function of the absolute temperature T by the equation

$$\log_{10}K=-21200/T+1.765\log_{10}T -9.85\times10^{-5}T-0.265, \tag{12}$$

as calculated by Bonhoeffer[36] from data of Langmuir. Writing

$$P(H)=XP, \tag{13}$$

where P is the total pressure,

$$P=P(H)+P(H_2), \tag{14}$$

we have the fractional dissociation, X, determined by the equation

$$X^2/(1-X)=K(T)/P. \tag{15}$$

In Fig. 5, X is shown as a function of T for several pressures.

[30] E. A. Hylleraas, Zeits. f. Physik **71**, 739 (1931); R. D. Present, J. Chem. Phys. **3**, 122 (1935); Coolidge, James, and Present, J. Chem. Phys. **6**, 730 (1938).

[31] W. Bleakney, Phys. Rev. **35**, 1180 (1930). H. F. Newhall, Phys. Rev. **62**, 11 (1942) has questioned this interpretation, but his apparatus may have discriminated against slow protons.

[32] W. E. Lamb, Jr. and R. C. Retherford, Phys. Rev. **75**, 1332 (1949).

[33] P. S. Olmstead and K. T. Compton, Phys. Rev. **22**, 559 (1923).

[34] O. S. Duffendack, Phys. Rev. **20**, 655 (1922); K. T. Compton, J. Opt. Soc. Am. **6**, 910 (1922).

[35] Davis, Feld, Zabel, and Zacharias, Phys. Rev. **76**, 1076 (1949).

[36] K. F. Bonhoeffer, Ergeb. d. exakt. Naturwiss. **6**, 201 (1927); also Wooley, Scott, and Brickwedde, J. Research Nat. Bur. Stand. **41**, 379 (1948).

No direct measurement of pressure in the tungsten oven could be conveniently made, but from the observed variation of yield with temperature when the experiment was successful, it seems reasonable that it was about 10^{-3} atmosphere in a typical case, and that the dissociation was 64 percent complete at $T=2500°K$. At this temperature, the most probable velocity in the beam is 8×10^5 cm/sec. for hydrogen atoms.

9. Excitation of Hydrogen Atoms by Electron Bombardment

The cross section for various electron excitation processes in hydrogen have been calculated by Bethe[37] according to the Born approximation, with neglect of electron exchange. Although this approximation is not expected to be very good for electron energies near the threshold, it was the only one available for our numerical estimates. The cross sections are given by

$$\sigma_{nl}=(8\pi hcR/mv^2)\,|\,(nl\,|\,x\,|\,10)\,|^2 \times[F_{nl}(y_{\max})-F_{nl}(y_{\min})] \quad (16)$$

where

$$y=1+(n/n+1)^2(Q/hcR)$$

$$F_{20}(y)=-(5y^5)^{-1}$$

$$F_{21}(y)=\log_e[(y-1)/y]+\sum_{s=1}^{5}(sy^s)^{-1}$$

$$F_{31}(y)=F_{21}(y)-(4/3y^6)+(4/7y^7)$$

$$Q_{\max}=(E^{\frac{1}{2}}+[E-E_{nl}+E_{10}]^{\frac{1}{2}})^2$$

$$Q_{\min}=(E^{\frac{1}{2}}-[E-E_{nl}+E_{10}]^{\frac{1}{2}})^2$$

E = electron energy,

E_{nl} = energy of atomic state.

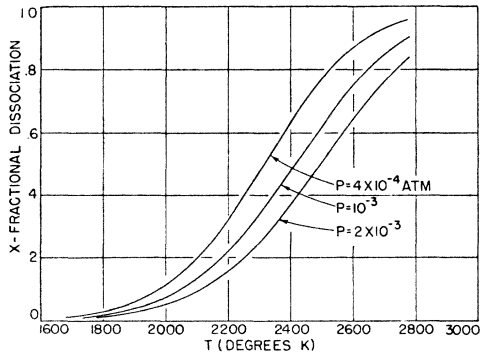

FIG. 5. Thermal dissociation of molecular hydrogen.

These cross sections are plotted as functions of electron energy in Fig. 6. The maximum cross section for $2s$ ($\sigma_{\max}=2.2\times10^{-17}$ cm^2) is about one-ninth that for $2p$, while that for $3p$ is smaller than that for $2s$ by a factor of 11. As a result, the yield of $2s$ by cascade from $3p$ may be neglected. The maximum yield for $2s$ comes at 14.8 volts, but does not fall below half the maximum value down to 11 volts.

Besides the errors inherent in the Born approximation, the neglect of electron exchange may be particularly serious for excitation of the optically inaccessible state $2s$, and one may hope to obtain a much larger cross section with a maximum nearer the threshold if exchange is included. Since no reliable calculations of exchange excitation, even with the Born approximation, seem to exist for hydrogen, we used the lower cross section $\sigma=10^{-17}$ cm^2, hoping to be on the save side.

If the detector is photo-sensitive there will also be a signal with the same threshold energy of 10.2 ev due to the Lyman photons from atoms excited to the $2p$ states. Any residual pressure of molecular hydrogen will also give photons. The threshold energy for the latter process is about 11.5 ev. Only a small fraction of these photons can reach the detector, but any background effects are undesirable.

10. Recoil Due to Bombardment

In the usual form of atomic beam experiment, one works with a very well-collimated beam. In the present case, it is necessary to bombard the hydrogen atoms after they leave the source, since Stark quenching must be minimized. One must then choose between bombardment at right angles to the beam, along it, or against it. The last two methods would not destroy the unidirectionality of the beam of atoms if the bombardment were at a voltage just above the threshold. Such a choice would be natural for other atoms, but not for metastable hydrogen atoms. In this case, one would be forced to have the magnetic field parallel to the electron beam. If the electrons were sent against the atomic beam, the metastable atoms would subsequently pass through an electric field which would quench them. If the electrons were sent along the beam, they could not easily be kept

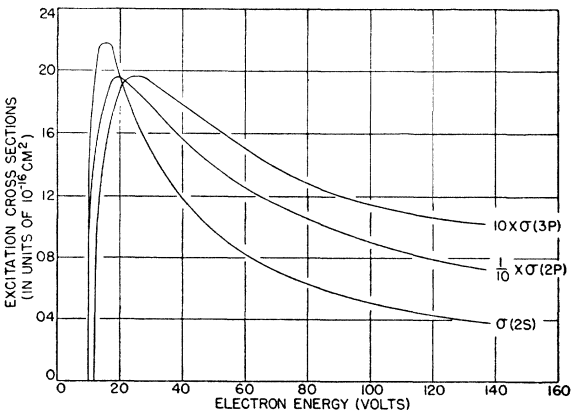

FIG. 6. Electronic excitation cross sections for states of atomic hydrogen calculated by Born approximation without exchange.

[37] See reference 25, p. 507.

from the detector. Methods based on difference in time of flight were rejected on intensity grounds.

The first choice necessarily leads to a transverse recoil, and what is worse, an indefinite one, so that an originally well-collimated beam is diffused by the bombardment. This means that the use of slits of the order of 0.001 in. width as in the usual atomic beam work is ruled out. On the other hand, one does not have the problem met there of detecting the small deflections of the beam in inhomogeneous magnetic fields, since the effect of the radiofrequency is much more easily distinguished here by the removal of the excitation of the absorbing atom.

The distribution of recoil angles is calculated in Appendix III and the results for typical cases are shown in Fig. 7. Even at the threshold, there is a distribution in horizontal recoil angle ranging (with larger than half the maximum probability) from 4° to 8.7° because of the distribution of velocities in the atomic stream. At 13.6 ev, the distribution broadens to range from 3.6° to 10.8°, and there is a distribution of vertical recoil angles between ±3.4°.

11. Detection of Metastable Hydrogen Atoms

The atoms excited by the electron bombardment to the metastable $2^2S_{1/2}$ state are supposed to move off to a suitable detector. Several possible methods of detection were considered. Two of these had been used previously to detect metastable atoms other than hydrogen. It was discovered by Webb[38] in 1924 that metastable atoms of mercury could eject electrons from metals. Later work by Oliphant[39] showed that the same was true of helium metastable atoms. A theory of this process was given by Massey,[40] and by Cobas and Lamb.[41] If the excited atom comes close to the surface of a metal, it may be energetically possible for a collision of the second kind to occur in which the atom returns to the ground state and an electron is liberated from the system to take up the excess energy. One possibility for such a process is shown in Fig. 8. The energetic condition for this is that the excitation energy, I, of the atom should exceed the work function, ϕ, of the metal. In the case of helium, the excitation energy is about 20 ev and the condition should be satisfied for all metals. In the case of mercury, the excitation energy of the 2^3P_0 state is only 4.68 volts, and the condition becomes much more critically dependent on the work function of the surface. In fact, Sonkin[42] showed in 1933 that the efficiency of detection of mercury metastables was very sensitive, by a factor of 100 or more, to the presence of surface contaminations. On the other hand, Dorrestein[43] in 1942 found that the efficiency of detection of helium metastables on outgassed platinum was about 40 percent and was subject only to relatively small fluctuations over a day's run. No information was available on the detection of hydrogen metastables. In this case, however, the excitation energy, 10.2 volts, is well above the work functions of metals, and one would at first expect a high efficiency of detection as with helium.

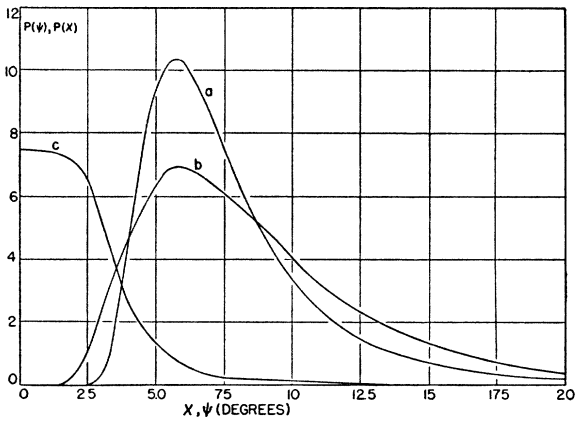

FIG. 7. Distributions in recoil angles. Curve (a): distribution in horizontal recoil angles ψ experienced by a hydrogen atom excited to the $2s$ state by electrons of energy just above the threshold. The temperature of the source of atoms is taken to be 2600°K. The total probability would be unity if the angle were measured in radians. Curves (b) and (c): distributions in horizontal recoil angles ψ and vertical recoil angles χ for hydrogen atoms excited to $2s$ by electrons of energy 13.6 ev.

According to rough calculations of the type mentioned above, metastable hydrogen atoms of thermal energy moving in toward a metal surface should, on the average, cause electron ejection before the atom reaches a distance of 2A. Since half of the electrons emitted probably go into the metal, one might expect an efficiency of the order of 50 percent.

Nevertheless, we were not very confident about the possibility of detecting hydrogen metastables by the above mechanism. These doubts arose in the following way: we were also considering another method based on the observation by Buehl[44] that metastable atoms of mercury falling on hot molybdenum are re-emitted as ions. This process is essentially the surface ionization detection method used for molecular beams in which an alkali atom falls on a hot tungsten surface, an electron is captured by the metal, and the resulting ion is evaporated from the surface. Such a process can be represented as shown in Fig. 9, and may take place if the energy inequality

$$\phi > I \tag{17}$$

holds.

In the case of hydrogen atoms in the $2s$ state, the ionization potential $I = 3.4$ volts. Most surfaces which can be maintained under the conditions of the experi-

[38] H. W. Webb, Phys. Rev. **24**, 113 (1924).
[39] M. L. Oliphant, Proc. Roy. Soc. **A124**, 228 (1929).
[40] H. S. W. Massey, Proc. Camb. Phil. Soc. **26**, 386 (1930); **27**, 460 (1931).
[41] A. Cobas and W. E. Lamb, Jr., Phys. Rev. **65**, 327 (1944).
[42] S. Sonkin, Phys. Rev. **43**, 788 (1933).
[43] R. Dorrestein, Physica **9**, 433 and 447 (1942).
[44] A. Buehl, Helv. Phys. Acta **6**, 231 (1933).

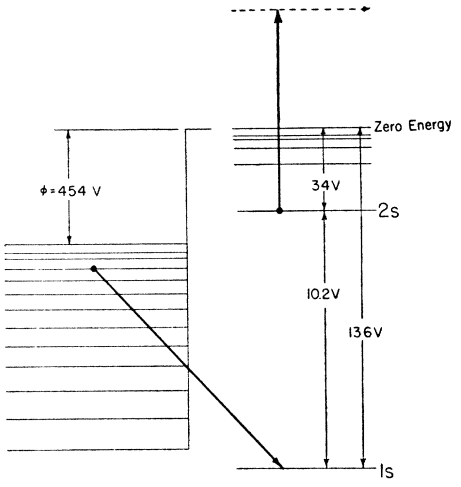

FIG. 8. A possible mechanism for ejection of electrons from tungsten by metastable hydrogen atoms due to the Coulomb interaction between the atomic and metallic electrons.

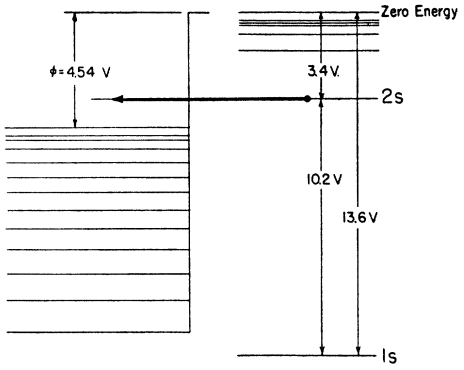

FIG. 9. Auto-ionization of a metastable hydrogen atom in the vicinity of a tungsten surface.

ment would probably have a work function $\phi > 3.4$ volts, and capture of the $2s$ electron by the surface is energetically possible. A rough estimate of the mean distance at which the process would occur gives 5A, i.e., a larger distance than that estimated for electron ejection. If the resulting proton could escape from the surface with appreciable probability, one would have a method for detecting metastable hydrogen atoms. If, however, the proton is neutralized in some way not involving electron emission, the process of electron capture might very well compete seriously with the desired process of electron ejection. When our experiment was successful, we found that electron ejection did occur, but probably not with the expected high efficiency. We have looked unsuccessfully for positive ion emission by metastable hydrogen atoms from cold and non-outgassed tungsten. Further investigation of the detection mechanism is clearly desirable.

We consider briefly, but did not attempt, methods involving the detection of the Lyman alpha 1216A radiation when a quenching field is applied to the beam or to the bombardment region.[45] Such a method would fit in well with the use of counters. Another possibility involving counters, which was not explored, would be to use secondary multiplication of the electrons ejected by the metastable atoms.

12. Estimate of Yield

We are now in a position to make a rough estimate of the yield of metastable hydrogen atoms and the resulting electron currents to be expected under typical experimental conditions. Consider the atoms emerging from the tungsten oven. According to ideal kinetic gas theory, the number of hydrogen atoms escaping per second at an angle θ with the normal to the wall into a solid angle range Ω through a small opening of area a is

$$\text{rate of escape} = n_0 a v \Omega X \cos\theta / 4\pi, \tag{18}$$

where n_0 is the number of atoms and molecules per unit volume, X is the fractional dissociation, and v is an average velocity of the atoms in the oven.

Few of these atoms can reach the detector plate directly, because it is offset to allow for the small recoil angle. If, however, it were not so displaced, and no obstacles were in the way, a fraction of the atoms emerging from the oven slit would reach the detector of area A at a distance R from the slit. For this, $\Omega = A/R^2$ and $\cos\theta \sim 1$. Let f be the fraction of atoms which are excited to the $2s$ state as they pass through the electron gun region. The excited atoms experience a deflection approximately sufficient to allow them to strike the displaced detector target. As there is a spread of recoil angles, the metastable atoms may not necessarily all be able to reach the detector. Only if the solid angle Ω_1 subtended by the detector seen through the slit system from the center of the bombardment region is larger than the solid angle Ω_2 of the beam spread due to recoil will the metastable atoms clear the intervening slit system. Otherwise only a fraction δ of these, called the "recoil dilution" factor, may do so. One may then set

$$\delta = \begin{cases} \Omega_1/\Omega_2 & \Omega_1 < \Omega_2 \\ 1 & \Omega_1 \geqslant \Omega_2. \end{cases} \tag{19}$$

The number of electrons/sec. ejected from the target due to metastable atoms is then

$$S = n_0 a v X A f \delta \mu \eta / 4\pi R^2, \tag{20}$$

where the factor μ expresses the fraction of metastables surviving their passage through any quenching electric fields, and η is the efficiency of the electron ejection by a metastable hydrogen atom from the metal surface used in the target.

The bombardment efficiency f may be estimated as follows: Let the electron stream have I electrons/sec.,

[45] This method was subsequently used by M. Skinner and W. E. Lamb, Jr., Phys. Rev. **75**, 1325 (1949); **78**, 539 (1950) for a determination of the fine structure anomaly in singly ionized helium.

a height h, and a width w. It takes a time w/v for an atom of speed v to pass through the bombardment region. The transition rate for an excitation process having a cross section σ is $I\sigma/wh$ so that the probability of excitation is

$$f=I\sigma/hv=2.3\times10^{-8} \tag{21}$$

with the typical values of bombarding current of 200 μa, $\sigma=10^{-17}$ cm^2, $h=1$ cm, $v=8\times10^5$ cm/sec., so that about one in forty million atoms is excited to the $2s$ state on passage through the bombardment region.

The detector signal is finally

$$S=n_0aXAI\sigma\delta\mu\eta/(4\pi R^2h) \text{ electrons/sec.} \tag{22}$$

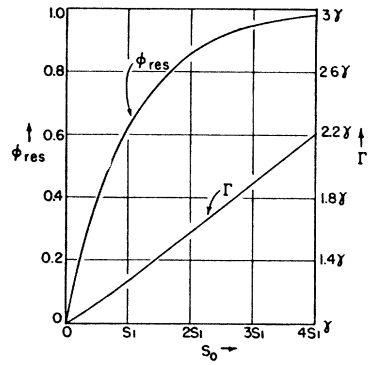

FIG. 10. Effects of r-f saturation. Resonance quenching and half-width as function of r-f power as given by Eqs. (28) and (25).

Unfortunately, many of the factors needed for the estimate of the yield were not known, and a certain degree of optimism was required in the assumption of relatively favorable values for then in order to predict a usable signal. Typical values were

$$\begin{aligned} &I=1.87\times10^{15} \text{ electrons/sec. (0.3 ma)}\\ &n_0=2.94\times10^{15} \text{ cm}^{-3} \text{ (10^{-3} atmos., 2500°K)}\\ &a=3.1\times10^{-3} \text{ cm}^2\\ &A=1.21 \text{ cm}^2\\ &R=6.35 \text{ cm}\\ &\sigma=10^{-17} \text{ cm}^2\\ &h=1 \text{ cm}\\ &X=0.64\\ &\delta=0.5\\ &\mu=0.5\\ &\eta=0.5. \end{aligned} \tag{23}$$

The values for a, A, R, h, I, n_0, and X were at least near the actual values used. As explained above, the value for σ was based on very inadequate theory. The value $\mu=\frac{1}{2}$ for the metastable survival factor was reasonable [Section 16] provided quenching effects were not present, including those which might be due to contact potential differences, or of electric fields due to charges trapped on insulating surface contaminations. The detector efficiency $\eta=0.50$ was taken most optimistically. The value of the recoil dilution factor $\delta=\frac{1}{2}$ was obtained by considering the width of the distribution of recoil angles and the areas of the holes through which the deflected beam must pass. One may not make these openings too large, for then the size of the region over which uniform magnetic and radio-frequency fields must be maintained becomes excessive. Also, the background signal due to photons originating in the bombardment region is increased relative to the signal, since the photons are not restricted to a relatively small range of solid angles.

With the above assumptions, the signal is

$$\begin{aligned} S&=3.26\times10^7 \quad \text{electrons/sec.}\\ &=5.2\times10^{-12} \quad \text{amp.} \end{aligned} \tag{24}$$

This is a current which is about 5×10^4 times the least current (10^{-16} amp.) which can be detected conveniently with an FP54 electrometer circuit and a sensitive galvanometer. Consequently, unless one or more of the estimates proved to be too optimistic, the signal should be large enough to detect, and even to use for accurate radiofrequency spectroscopy. As will be seen later, this estimate proved to be very optimistic.

13. Radiofrequency Power Required

The metastable atoms are to be subjected to radio-frequency waves somewhere between the source and detector. When the frequency is such that $\hbar\omega$ is equal or nearly equal to an energy difference between a Zeeman component of the $2^2S_{1/2}$ level and a Zeeman component of one of the 2^2P levels, the radiation may induce a transition to a non-metastable level and the detected signal will decrease. The amount of decrease will depend on the intensity of the radiation as well as its frequency, on the speed of the atoms, and the length of the radiofrequency field region. We will now estimate the amount of r-f power required for an appreciable quenching of the beam.

According to the quantum theory of radiation, the decay rate of state $2^2S_{1/2}$ to one of the $2p$ states due to r-f is[46]

$$1/\tau_s=(2\pi e^2\gamma S_0/c\hbar^2)\times|(|\hat{\mathbf{e}}\cdot\mathbf{r}|)|^2/[(\omega-\omega_0)^2+(\gamma/2)^2], \tag{25}$$

where S_0 is the incident energy flux density of the radiation having circular frequency ω and electric polarization parallel to the unit vector $\hat{\mathbf{e}}$, ω_0 is the resonance circular frequency and $(|\mathbf{r}|)$ is the matrix element of the coordinate vector $\mathbf{r}$ for the transition in question. As before, $\gamma=1/\tau_p$ is the radiative damping constant for $2p$ states. At resonance, $\omega=\omega_0$ and

$$1/\tau_s=(8\pi e^2S_0/c\hbar^2\gamma)|(|\hat{\mathbf{e}}\cdot\mathbf{r}|)|^2. \tag{26}$$

The matrix elements of $\hat{\mathbf{e}}\cdot\mathbf{r}$ can be calculated from equations[47] given by Bethe, and for a transition from $2^2S_{1/2}$ ($m=\frac{1}{2}$) to $2^2P_{1/2}$ ($m=-\frac{1}{2}$) with $\hat{\mathbf{e}}$ along x we find

$$|(|x|)|^2=3a_0^2. \tag{27}$$

[46] The validity of Eq. (25) will be discussed in a later paper.
[47] See reference 25, p. 447.

The fraction of atoms quenched by the r-f field is

$$\phi = 1 - \exp(-l/v\tau_s), \tag{28}$$

where l is the length of the r-f region, and v is the speed of the atoms. For $l=1$ cm and $v=8\times10^5$ cm/sec., the beam would be 63 percent quenched for

$$\tau_s = l/v = 1.25\times10^{-6} \text{ sec.} \tag{29}$$

According to Eq. (26) this requires an energy flux density at resonance of $S_0=3.4$ mw/cm^2. Since this power density is easily obtained at any frequency up to 30,000 Mc/sec., we did not anticipate any difficulty with r-f power requirements.

It is clear from Eqs. (28) and (25) that when the r-f power is sufficient to give nearly complete quenching at resonance, the effective resonance curve will be appreciably broadened by r-f saturation. The dependence of quenching and effective half-width Γ on r-f power is shown in Fig. 10.

14. Breadth of Resonance Curves

According to Eq. (25), the decrease in the beam will take place when $\omega=\omega_0$ and also for a band of frequencies around $\omega_0/2\pi$ of half-width $\gamma/2\pi$ or 99.8 Mc/sec. This is just the uncertainty principle width ($\Delta E\Delta t\sim\hbar$) of the decaying 2^2P states and cannot be reduced. In addition, as we shall see later, hyperfine structure increases the width of the lines by as much as a factor of two in some cases. The large width of the resonance curves is a significant fraction of the frequencies of the transitions, and represents the greatest difficulty in the way of a really precise test of the Dirac theory. On the other hand, an opportunity is afforded for a quite accurate test of the Wigner-Weisskopf theory of radiation line

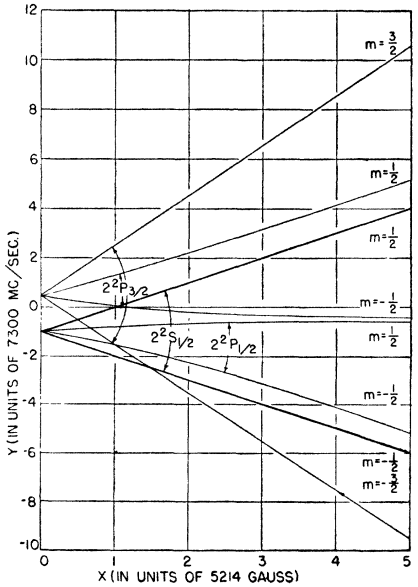

FIG. 11. Zeeman splitting of the fine structure of states $n=2$ of hydrogen according to the Dirac theory.

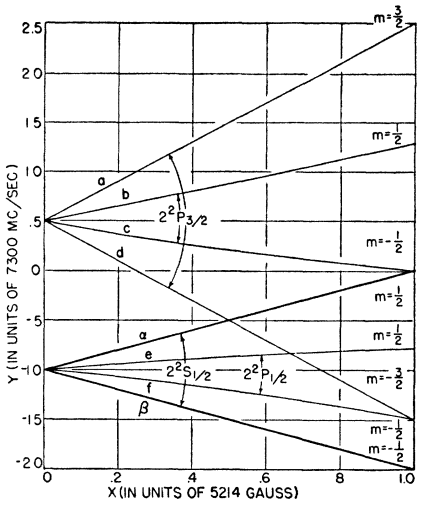

FIG. 12. Enlargement of Fig. 11 showing abbreviations used for the Zeeman component energy levels.

shape, since the resonance curves have a natural width relative to the working frequency much greater than elsewhere in atomic physics.

The most obvious way to determine the resonance frequencies $\omega_0/2\pi$ would be to measure the beam intensity as a function of radiofrequency, keeping the r-f power constant. Unfortunately, this is next to impossible to do. Microwave oscillators which can be tuned through hundreds of megacycles per second are available, but their output is frequency-dependent. Even if this were not the case, the transmission line or wave guide to the quenching region would be electrically long and unless the line were very well broad-banded, the standing wave ratio, and hence the r-f voltage seen by the atom would vary with frequency. One might hope to monitor the r-f power level with a crystal probe or bolometer mounted in the quenching region, but such devices are themselves frequency-sensitive.

Since a magnetic field was believed to be necessary anyway, we decided to take advantage of it to overcome the above difficulties. The frequency (and power level) of the oscillator is kept constant and the atomic energy levels are moved through resonance by varying the magnetic field. To a first approximation, the atomic energies, and therefore the frequencies, are linear functions of the magnetic field, so that a resonance curve taken in this way closely resembles in shape the usual sort. In order to interpret the result, however, it is necessary to know the values of the magnetic field and to have the theory of the Zeeman effect of the hydrogen fine structure levels for $n=2$. The results of this theory are summarized in the next section.

15. Zeeman Effect of the Fine Structure of Hydrogen

For the present, it will suffice to consider an approximate theory of the Zeeman effect of the hydrogen fine

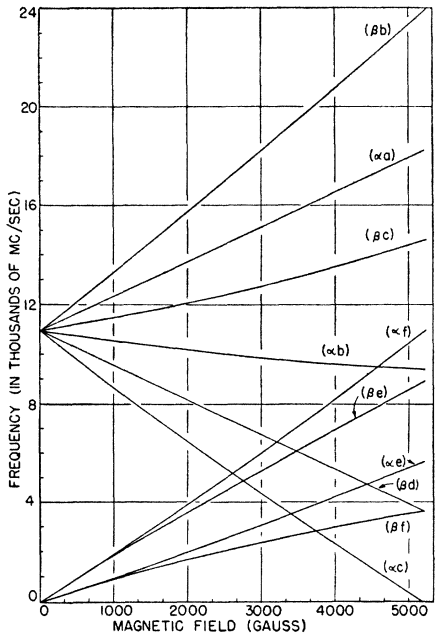

FIG. 13. Resonance frequencies to be expected as functions of magnetic field for all allowed transitions leading from the metastable states $\alpha(2^2S_{1/2},\ m=\frac{1}{2})$ and $\beta(2^2S_{1/2},\ m=-\frac{1}{2})$ to the non-metastable states a, b, c, d $(2^2P_{3/2})$ and e, f $(2^2P_{1/2})$ according to the Dirac theory.

structure in which the interaction of the atom with an external magnetic field H is represented by the perturbing energy

$$\mathcal{H}'=\mu_0(\mathbf{L}\cdot\mathbf{H}+2\mathbf{S}\cdot\mathbf{H}), \tag{30}$$

where

$$\mu_0=e\hbar/2mc \tag{31}$$

is the Bohr magneton, $\mathbf{L}=(\mathbf{r}\times\mathbf{P})/\hbar$ the orbital angular momentum, and $\mathbf{S}$ the spin angular momentum of the electron, measured in units of $\hbar$. The splitting of the $2^2S_{1/2}$ levels may be considered independently of that of the 2^2P levels for $\mathcal{H}'$ has no matrix elements connecting s and p states. The solution of this problem is well known, and we simply take the results[48] from Bethe's article.

For $2^2S_{1/2}$, $m_s=\pm\frac{1}{2}$

$$E(2^2S_{1/2},\ m_s;\ H)=E(2^2S_{1/2})+2\mu_0Hm_s. \tag{32}$$

For $2^2P_{3/2}$, $m_j=\pm\frac{3}{2}$

$$E(2^2P_{3/2},\ m_j=\pm\tfrac{3}{2};\ H)=E(2^2P_{3/2})+(4/3)\mu_0Hm_j. \tag{33}$$

For the $m_j=\pm\frac{1}{2}$ levels of $2^2P_{1/2,\,3/2}$ the levels are given by the roots of a secular determinant as

$$E=\tfrac{1}{2}(E_++E_-)+\mu_0Hm_j \pm\tfrac{1}{2}[(E_+-E_-)^2+(4/3)\mu_0H(E_+-E_-)m_j+(\mu_0H)^2]^{\frac{1}{2}} \tag{34}$$

where E_+ and E_- are the zero field energies of $2^2P_{3/2}$ and $2^2P_{1/2}$ respectively.

[48] See reference 25, p. 396.

If we measure energy in units of

$$hf_1=2(E_+-E_-)/3\cong 7300 \text{ Mc/sec.} \tag{35}$$

from the center of gravity $\frac{1}{3}(2E_++E_-)$ and magnetic field in units

$$H_1=(2/3\mu_0)(E_+-E_-)\cong 5214 \text{ gauss} \tag{36}$$

by setting

$$\mu_0H=\tfrac{2}{3}(E_+-E_-)x \tag{37}$$

$$E=\tfrac{2}{3}(E_+-E_-)y+\tfrac{1}{3}(2E_++E_-), \tag{38}$$

we obtain

$$y=-\tfrac{1}{4}+m_jx\pm\tfrac{1}{2}(x^2+2m_jx+9/4)^{\frac{1}{2}}. \tag{39}$$

In the same notation, the energy levels for $2^2P_{1/2}$, $m=\pm\frac{3}{2}$ are given by

$$y=\tfrac{1}{2}\pm 2x \tag{40}$$

and for $2^2S_{1/2}$, $m_s=\pm\frac{1}{2}$

$$y=y_0-1\pm x \tag{41}$$

where y_0 measures any displacement upward of $2^2S_{1/2}$ compared to $2^2P_{1/2}$ in zero magnetic field. A plot of these energy levels is given in Fig. 11 showing the anomalous Zeeman, intermediate field, and Paschen-Back regions. Here $y_0=0$ as predicted by the Dirac theory. For the sake of brevity, these energy levels will be denoted by single letters. The two metastable levels $2^2S_{1/2}$, $m_s=\frac{1}{2}$ and $m_s=-\frac{1}{2}$ will be denoted by α and β, respectively (as suggested by the conventional symbols for Pauli spin wave functions). The 2^2P levels will be denoted by a, b, c, d, e, f as shown in Fig. 12 which enlarges the anomalous Zeeman and intermediate field regions of primary interest to us.

The selection rules for electric dipole radiation in the anomalous Zeeman region are $\Delta m_j=0$ for the electric vector of the radio waves parallel to the magnetic field, and $\Delta m_j=\pm 1$ for perpendicular polarization. Conse-

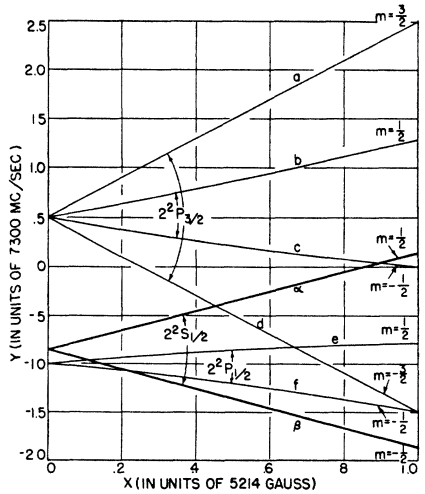

FIG. 14. Zeeman energy levels as in Fig. 11, but with the $2^2S_{1/2}$ pattern raised by 1000 Mc/sec.

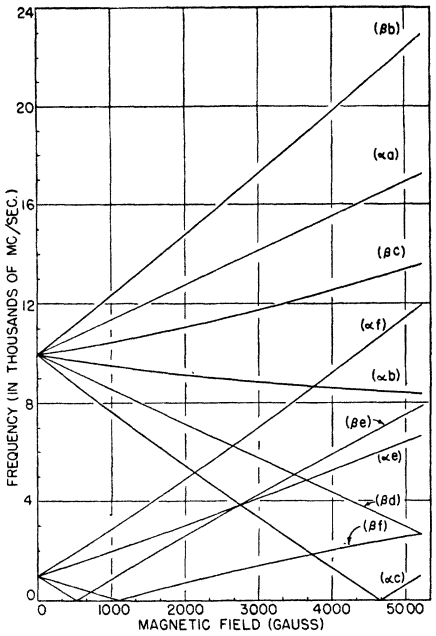

FIG. 15. Expected resonance frequencies as functions of magnetic field as in Fig. 13, but with the $2^2S_{1/2}$ state raised by 1000 Mc/sec.

quently, for parallel polarization the allowed transitions are αb, αe, βc, βf while for perpendicular polarization the allowed transitions are αa, αc, αf, βb, βd, βe. The frequencies to be expected for these ten transitions are plotted in Fig. 13 as a function of the magnetic field.

In actuality, taking the fine structure separation $\alpha^2 hcR/16$ as 10, 950 Mc/sec. and the s level shift Δ as 1000 Mc/sec., we now know that $y_0 \sim 0.137$ and not zero as predicted by the Dirac theory. On this basis the energy level curves are as shown in Fig. 14. The corresponding frequency *versus* field curves are shown in Fig. 15.

16. Production of a Polarized Beam of Atoms

It will be noted from a comparison of Figs. 12 and 14 that the existence of the $2^2S_{1/2}$ level shift gives rise to a marked difference in the stability of the two metastable states α and β in magnetic fields of around 540 gauss. For the quenching effect of an electric field $\mathbf{E}$ is given by

$$1/\tau_s = \gamma V^2/\hbar^2[\omega^2 + (\tfrac{1}{2}\gamma)^2], \tag{42}$$

where $V = (|e\mathbf{E}\cdot\mathbf{r}|)$ is the matrix element of the perturbation $e\mathbf{E}\cdot\mathbf{r}$ connecting the two interacting states, and $\hbar\omega$ is their energy difference. At 540 gauss, $\omega/2\pi$ is 2020 Mc/sec. for the separation between states αf and zero for the states βe. As a result, the quenching of the lower metastable state β will be more rapid than that of the upper state α by a factor of

$$1 + (4\omega^2/\gamma^2) \sim 1630. \tag{43}$$

The main known perturbing electric field is that due to the motion of the atoms at right angles to the magnetic field $\mathbf{H}$, and is given by

$$\mathbf{E} = (\mathbf{v}/c) \times \mathbf{H}. \tag{44}$$

Hence $\mathbf{E}$ is perpendicular to $\mathbf{H}$. If we introduce a right-handed Cartesian coordinate system with z along $\mathbf{H}$, x along $\mathbf{v}$, then $\mathbf{E}$ is along y. The perturbation energy $e\mathbf{E}\cdot\mathbf{r}$ has matrix elements connecting states β and e, but not states β and f. For $v = 8\times10^5$ cm/sec. and $H = 540$ gauss, $E = 4.3$ volts/cm.

The life of state β in a perturbing electric field of 4.3 volts/cm perpendicular to the magnetic field is given by Bethe's calculations as described in Section 6 to be 4.3×10^{-8} sec. while state α would have a life 1630 times greater, or 7×10^{-5} sec. This means that in the presence of the motional electric field, atoms in state α will nearly all be able to keep their excitation while they travel 6 cm to a detector, but practically none of the atoms originally in the lower metastable state β will be excited when they reach the detector. Hence, after moving a short distance along the beam from the electron bombarder, we will have a polarized beam of atoms, nearly all the excited atoms having electron spins oriented parallel to the magnetic field. The excited atoms with antiparallel spins have been filtered out by the quenching action of the motional electric field. This method of production of a highly polarized beam of matter is to be contrasted with the other known methods: the small spatial separations obtained in atomic beam deflection experiments, and the polarization of neutrons on passage through strongly magnetized absorbers.

The state of affairs described above is not confined to the critical field of $H = 540$ gauss for which the levels β and e cross, but extends over quite a range of field strengths. With the apparatus to be described in this paper, the transitions βb, βc, βd, βe, βf of Fig. 15 were not observed.

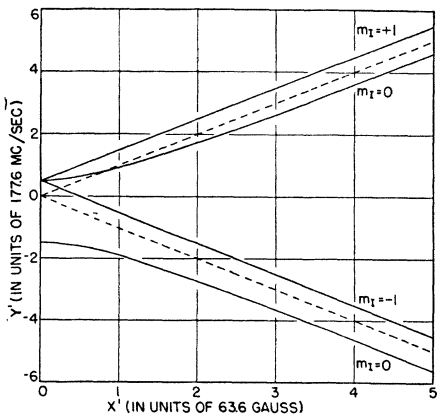

FIG. 16. Zeeman splitting of the hyperfine structure of $2^2S_{1/2}$. The zero-field separation is taken to be one-eighth that measured for the ground state by Nafe and Nelson. The dotted lines show the energy levels obtained if hyperfine structure is ignored.

Motional Stark quenching also occurs about the magnetic field where levels α and c cross, or $H=4700$ gauss. This region is much wider than for the βe crossing because the motional electric field is larger, and the beam of metastable atoms will be strongly quenched above 3000 gauss.

17. Effect of Hyperfine Structure of Energy Levels

The discussion of the energy levels of the $n=2$ states in Section 15 ignored the interaction of the magnetic moment of the nucleus (proton, deuteron, $\cdots$) with the electron. Fortunately, although the effects of this are not negligible by any means, they can be taken into account by perturbation theory for the purposes of the present discussion. The magnetic moment of the nucleus

$$\mathfrak{y}=g_I\mathbf{I}\mu_0 \tag{45}$$

produces a magnetic field derivable from the vector potential

$$\mathbf{A}=(\mathfrak{y}\times\mathbf{r})/r^3. \tag{46}$$

Here g_I is the Landé value for the nucleus (about 5.6/1836 for the proton and 1.7/1836 for the deuteron), μ_0 is the Bohr magneton (31) and $\mathbf{I}$ is the spin vector for the nucleus. According to Dirac's equation, the interaction energy with the electron is $e\boldsymbol{\alpha}\cdot\mathbf{A}$ where α_x, α_y, α_z are the Dirac matrices. The shift of the energy levels due to hyperfine structure is small and can be calculated using first-order perturbation theory by forming the average of $\boldsymbol{\alpha}\cdot\mathbf{A}$ over the unperturbed Dirac four-component wave function for the state of the electron. In forming this average, the two small component wave functions must be calculated with some care near the nucleus in order to avoid ambiguities due to the singularity at the origin in $\mathbf{A}$. The theory[49] is conveniently worked out by Bethe for the case of vanishing external magnetic field. The results for the energies are given below.

For s states the effective perturbation operator is

$$w=(16\pi/3)g_I\mu_0^2|\psi(0)|^2\mathbf{I}\cdot\mathbf{S} \tag{47}$$

or

$$w=(8/3)g_I(Z^3/n^3)\alpha^2hcR\mathbf{I}\cdot\mathbf{S} \tag{48}$$

giving energy shifts

$$=(4/3)g_I(Z^3/n^3)\alpha^2hcR\begin{cases} I & \text{for } F=I+\frac{1}{2} \\ -(I+1) & \text{for } F=I-\frac{1}{2}. \end{cases} \tag{49}$$

The separation of the two states is

$$\Delta w_n=(8/3)g_I(I+\tfrac{1}{2})(Z^3/n^3)\alpha^2hcR. \tag{50}$$

For the ground state of hydrogen, this splitting amounts to 1416 Mc/sec., (increased to 1420 Mc/sec. by the anomalous magnetic moment of the electron as shown through the work of Nafe, Nelson, and Rabi[50]). For the case $n=2$, of interest to us, the splitting is one-eighth as much, or 177 Mc/sec.

The theory of the Zeeman effect of this hyperfine structure for all magnetic fields is given by the well-known Breit-Rabi[51] formula, and is illustrated in Fig. 16. For present purposes it suffices to consider only the strong field limit in which $\mathbf{I}$ and $\mathbf{S}$ are decoupled from each other and precess independently around H with projections m_I and m_s, respectively. Then $\mathbf{I}\cdot\mathbf{S}$ can be replaced by m_Im_s and we obtain for the hyperfine energy

$$w=(8/3)g_I(Z^3/n^3)\alpha^2hcRm_Im_s. \tag{51}$$

State α, for which $m_s=+\frac{1}{2}$ is therefore split into $2I+1$ states. For hydrogen, with $I=\frac{1}{2}$, there are two states separated by $(\frac{1}{2})\Delta w$ or 88 Mc/sec. State β, $(m_s=-\frac{1}{2})$ is similarly split, but with an inversion because of the sign change of m_s. In the interpretation of the more precise measurements to be described in a later paper, it will, of course, be necessary to question the validity of the strong field approximation. For the present purposes, the error is not large since the dimensionless parameter

$$x'=(g_J-g_I)\mu_0H/\Delta w \tag{52}$$

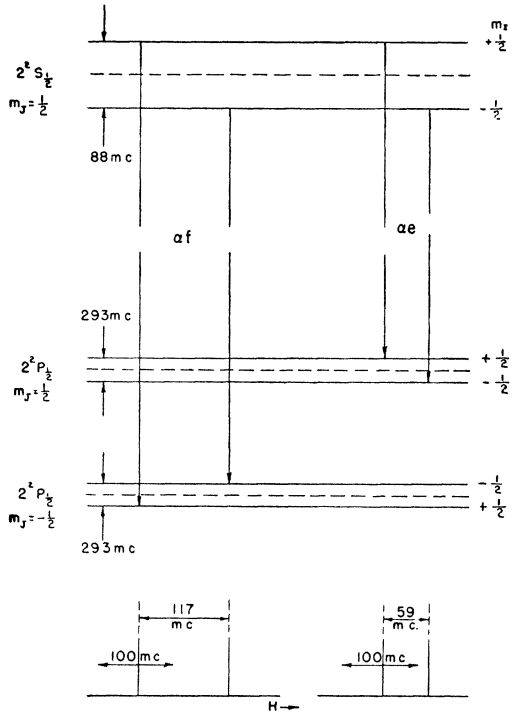

FIG. 17. Hyperfine structure of the $2^2S_{1/2}$ $(m=\frac{1}{2})$ and the $2^2P_{1/2}$ levels in strong magnetic field. The allowed transitions are indicated by the arrows. The resonance curve peaks are separated by 117 and 59 Mc/sec., respectively. This separation is to be compared with the radiative width of 100 Mc/sec. For simplicity, the hyperfine components have been taken to be equally separated from the dotted position corresponding to complete Back-Goudsmit decoupling.

[49] See reference 25, p. 385.

[50] J. E. Nafe and E. B. Nelson, Phys. Rev. **73**, 718 (1948); P. Kusch and H. M. Foley, Phys. Rev. **74**, 250 (1948).

[51] G. Breit and I. I. Rabi, Phys. Rev. **38**, 2082 (1931).

reaches unity at a magnetic field of only 63.6 gauss, and nearly all of the data described here was taken at fields well above this.

For other than s states, Bethe assumed that the fine structure splitting was large compared to the hyperfine structure separation and derived the equation

$$w=2\mu_0^2 g_I\langle r^{-3}\rangle_{Av}[L(L+1)/J(J+1)]\mathbf{I}\cdot\mathbf{J}$$
$$=g_I(Z^3/n^3)(\alpha^2 hcR)(\mathbf{I}\cdot\mathbf{J})/[(L+\tfrac{1}{2})J(J+1)] \quad (53)$$

for the perturbation operator. In zero magnetic field,

$$\mathbf{I}\cdot\mathbf{J}=\tfrac{1}{2}[F(F+1)-I(I+1)-J(J+1)] \quad (54)$$

and

$$(\mathbf{I}\cdot\mathbf{J})_{F=|I-J|}-(\mathbf{I}\cdot\mathbf{J})_{F=I+J}=\begin{cases} I(2J+1) & J\geqslant I \\ J(2I+1) & J<I \end{cases}$$

so that for hydrogen the state $P_{1/2}$ splits into two states with resultant angular momentum quantum number $F=1$, 0 and $P_{3/2}$ splits into two states with $F=2$, 1. The separations are, respectively, 1/3 and 2/15 as much as for the corresponding $2S_{1/2}$ state.

In the presence of a magnetic field which is not large enough to break down the coupling between **L** and **S** to form a resultant **J**, one may continue to use Eq. (53). However, one must add to the Hamiltonian the energy of orientation of the vectors **I** and **J** in the magnetic field

$$\mu_0(g_J\mathbf{J}-g_I\mathbf{I})\cdot\mathbf{H}$$

and the problem becomes mathematically similar to that of the Zeeman effect of the hfs for S states so that the Breit-Rabi formula may be used, if either I or J is $\frac{1}{2}$.

We obtain a simplification if we consider magnetic fields which are strong enough to decouple **I** from the vector **J**, but not strong enough to decouple **L** and **S**. Then $\mathbf{I}\cdot\mathbf{J}$ may be replaced by $m_I m_J$ and the hyperfine energy becomes

$$w=(g_I Z^3\alpha^2 hcR/n^3 J(J+1)(L+\tfrac{1}{2}))m_I m_J$$
$$+\mu_0 H(g_J m_J-g_I m_I). \quad (55)$$

As a result of the hyperfine structure, again taking the case $I=\frac{1}{2}$ for simplicity, each state is in effect split into two states equally removed in energy from the unperturbed position. To the approximation considered here, the hyperfine splittings are dependent on magnetic field only because of the last term $-\mu_0 H g_I m_I$ of Eq. (55). The splittings are expected to be $(\frac{1}{2})\Delta w=88$ Mc for the $2^2S_{1/2}$ states, $(1/6)\Delta w=29$ Mc for the $2^2P_{1/2}$ states while it is $(1/30)\Delta w=6$ Mc for the $m_J=\pm\frac{1}{2}$ states of $2P_{3/2}$, and $(1/10)\Delta w=9$ Mc for the $m_J=\pm\frac{3}{2}$ states of $2P_{3/2}$. For the case of deuterium, when $I=1$ the patterns are more complicated but the splittings are very much small because of the smaller nuclear magnetic moment.

The splitting of the energy levels due to hyperfine structure gives rise to a complication of the observed

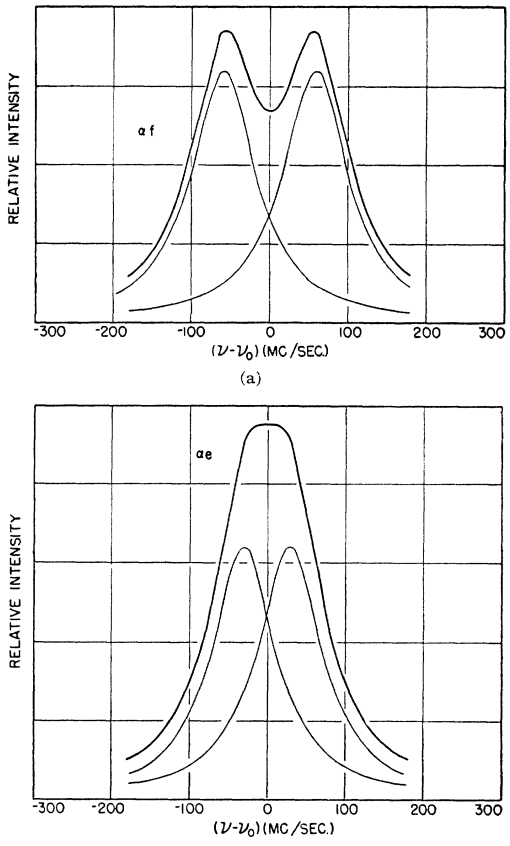

FIG. 18. Ideal theoretical resonance curves showing the effect of hyperfine structure for transitions αe and αf, respectively. When plotted as functions of magnetic field, the resonance curve for αf becomes the narrower of the two.

resonance curves. In most cases the natural width of the curves exceeds the splitting, and the result is a composite of two more or less imperfectly resolved resonance curves of the Wigner-Weisskopf type. The case of transitions from state $\alpha(2^2S_{1/2},\ m_s=\frac{1}{2})$ to states $e(2^2P_{1/2},\ m_j=\frac{1}{2})$ and $f(2^2P_{1/2},\ m_j=-\frac{1}{2})$ will serve to illustrate this. The observed transitions are electric dipole in type, and as the nuclear moment is decoupled from the other angular momentum vectors by the magnetic field, the selection rule $\Delta m_I=0$ obtains.

The allowed transitions are shown in Fig. 17. It will be noted that because of the reversal of sign of the product $m_I m_J$ the separation of the two peaks is $(4/3)\Delta w$ or 117 Mc/sec. for transition αf and only $(\frac{2}{3})\Delta w$ or 58 Mc/sec. for transition αf. The natural width of the separate transitions is 100 Mc/sec. When two such curves are superposed, the resulting complex has two peaks only if the component peaks are separated by half the natural width, or by 50 Mc/sec. The theoretical forms of such curves are shown in Fig. 18(a) and (b). Even in the case αf, where the separation is 117 Mc/sec., the result may be only a flattening of the top of the curve if there are other causes of

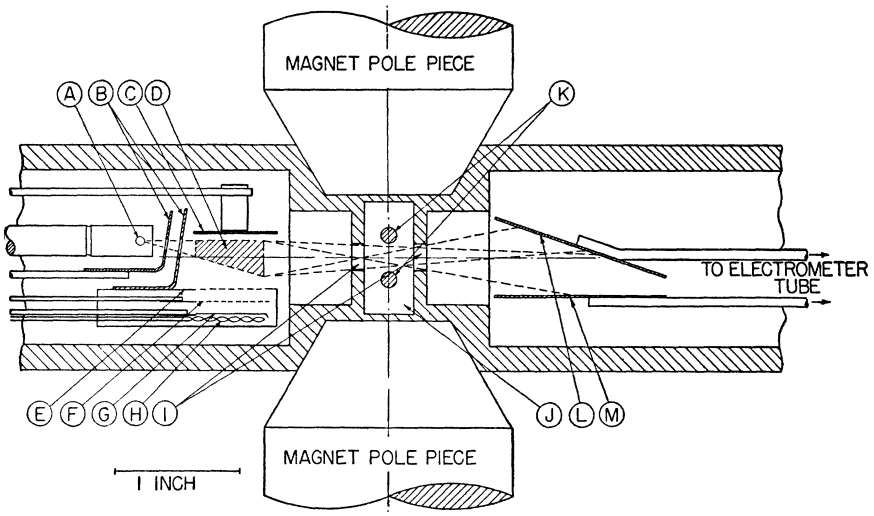

FIG. 19. Cross section of apparatus. A. Tungsten oven of hydrogen dissociator. B. Shields. C. Anode of electron bombarder. D. Bombardment region. E. Accellerator grid of electron bombarder. F. Control grid. G. Cathode of electron bombarder. H. Heater for cathode. I. Slits. J. Wave guide. K. Quenching wires and transmission lines. L. Metastable detector target. M. Electron collector.

broadening. In the work described in this paper, the observed peaks were considerably broader than expected above because of magnetic field inhomogeneity.

C. APPARATUS

18. Preliminary Efforts

Inasmuch as the production and detection of metastable hydrogen atoms were theoretically possible, but experimentally unproven, it was necessary at the outset to establish the occurrence of both processes simultaneously. The earliest apparatus was conceived as simply as possible consistent with this aim, as a source and detector of metastable atoms. These were enclosed in glass bulbs connected by a glass tube $\frac{1}{2}$ in. in diameter and 6 in. long. Magnetic fields could be applied to the source, detector, and intervening region. These were produced by permanent magnets of a type once used for K band magnetrons. It was thought that at a later time the connecting tube could be passed through the broad side of an X band wave guide (0.400×0.900 in. I.D.), so that the metastable atoms could be subjected to a radiation field having a frequency of about 10,000 Mc/sec.

The second method of Section 7, that of direct excitation by electron bombardment of the molecule, was selected as probably the easiest way to produce metastable hydrogen atoms. The electron bombarder consisted of an oxide-coated cathode, a grid and an anode. The latter two electrodes were held at the same positive potential with respect to the cathode to produce a relatively field-free region where metastable atoms could be formed. This arrangement was capable of supplying electrons with energies up to 50 ev.

For reasons discussed in Section 11, the electron ejection method of detection was adopted. The atoms were allowed to fall on a tungsten target and any electrons ejected passed to a positive collector electrode. This method has the disadvantage that electrons ejected from the surface by any other means, such as photoelectric effect, form a background which has to be held within reasonable bounds. However, the background photoelectric current made possible a study of the behavior of the electron bombarder by taking excitation curves for hydrogen and helium.

Hydrogen gas was admitted near the electron bombarder and if metastable atoms were formed, some would have passed through the connecting tube to the detector. Unfortunately, the bombardment of molecular hydrogen produced a variety of effects difficult to distinguish from those expected of metastable hydrogen. With the aid of the magnetic fields and an electric field produced by a pair of auxiliary electrodes introduced for that purpose into the connecting tube, it was shown that these phenomena could be attributed to photons, electrons, positive ions and charges accumulated on the glass walls. The last effect was particularly confusing.

The usual method of study at this stage was to take rough excitation curves as a function of the bombarding voltage, with proper allowance for the presence of extraneous ions, electrons and the effects of charges on the glass walls. Although at this time it was not possible to verify the presence of metastable atoms, it was

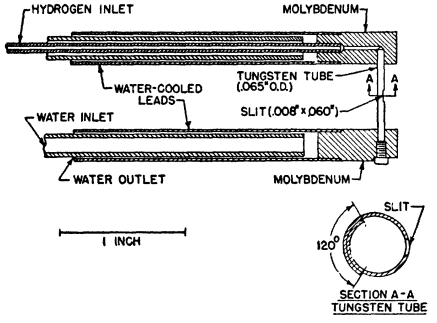

FIG. 20. Detail of hydrogen dissociator and tungsten oven.

evident from the size and low appearance potential of the photon background that the chosen excitation process was not as favorable as anticipated. It appeared that the two-step method of first dissociating the molecule and then exciting the atoms by electron bombardment would be less affected by this difficulty.

19. Working Model

Since it was clear that an extensive revision of the apparatus was necessary, a primarily all metal one was built incorporating all known improvements. Nevertheless, many modifications were made before meaningful results were obtained.

The general scheme of the apparatus is illustrated in Fig. 19 which is a horizontal cross section through the axis of the coaxial circular cylinders comprising the right- and left-hand chambers. The rectangular space, J, is the cross section of an X-band rectangular wave guide 0.400×0.900 in. I.D., which passes through the apparatus vertically. The magnetic field, neglecting fringing, is at right angles to both the wave guide and the right and left chambers. The magnet pole pieces fit into truncated conical indentations in the apparatus. Except for a certain amount of ferromagnetic material, such as steel and Kovar near the glass seals, the outer shell of the apparatus is principally composed of OFHC copper.

The right-hand chamber contains the detection electrodes and the left the hydrogen dissociator and the electron bombarder. The intervening chamber J is the r-f field region. Hydrogen atoms leave the hydrogen dissociator A and pass to the interaction space D where some of them are excited to the $2s$ state by electron bombardment. After experiencing a small recoil, they pass through the slits I and the r-f region to the detector target, L.

In agreement with the considerations discussed in Section 10 and in Appendix III, the recoil angle was taken into account in the choice of the relative positions of the hydrogen dissociator, the electron bombarder, and the slits I. The angle chosen was the average ψ for 13.6 ev. This is about 8° (see Appendix III).

20. Detector

The detection electrodes consist merely of two tungsten plates, L and M. In the manner described in Section 11 metastable atoms fall on L and eject electrons which are collected by M which is held 3 or 4 volts positive with respect to L. The electron current is measured by means of a standard FP54 electrometer circuit[52] with an input resistance of about 95,000 megohms. The current sensitivity was about 1.5×10^{-16} amp./mm. It was found that cleaning the target, which was at that time a tungsten ribbon 0.004 in. thick and $\frac{1}{4}$ in. wide, by heating to 1000°C or more had no lasting effect. Consequently, an unheated target was used with no apparent loss of sensitivity. The response to metastable atoms is not very sensitive to collector voltage so long as it is 2 or 4 volts but falls off rapidly when the potential difference is dropped toward zero, and becomes vanishingly small at negative values of a volt or so.

Inasmuch as the target surface was only superficially cleaned during assembly, it was very likely covered with a contaminating layer of some sort. In any case such layers frequently become visible after operation for a time, apparently without greatly affecting the detector efficiency.

21. Hydrogen Dissociator

Atomic hydrogen was produced by thermally dissociating molecular hydrogen as discussed in Section 8. The details of the arrangement are shown in Fig. 20. A thin-walled tungsten cylinder, 0.065 in. O.D., was fabricated from 0.004-in. tungsten sheet as indicated, and a slot 0.008×0.060 in. was cut near the center and parallel to the cylinder axis. The cylinder was then forced into the holes provided in the molybdenum ends of the water-cooled leads. Molecular hydrogen was introduced through a tube inside one of the water ducts. The tungsten tube could then be heated in its central portion to a temperature sufficient to produce a satisfactory degree of dissociation by the passage of electric current. The atoms so produced stream out of the small slot which serves as the source. Naturally, there is a fair amount of leakage of molecular hydrogen around the ends of the cylinder.

Operating temperatures in the central portion of the cylinder were usually about 2500°K. Higher temperatures, although possible and desirable, resulted in too high a mortality of the tungsten cylinders. No accurate data are available for the degree of dissociation so produced; however, on the basis of the estimate of Section 8, the degree of dissociation was about 64 percent. The disadvantage of working with this rather low degree of dissociation is outweighed by the general convenience of the method.

Alternating current was found to be satisfactory for heating the hydrogen dissociator. A current of 80 amp. and a voltage drop of 2 volts represent typical operating conditions. The transformer was stabilized by a Sola constant voltage transformer.

22. Electron Bombarder

The electron bombarder has proven to be the most troublesome part of the apparatus, and much effort was expended in determining how to make a good one. Inasmuch as considerably more work has been done on it in preparation for the more precise determination of the $2s$ level shift, this subject will be considered further in Part II.

From the discussions of Sections 6 to 10, it is quite possible to state the properties of an ideal electron gun

[52] L. A. duBridge and H. Brown, Rev. Sci. Inst. 4, 532 (1933).

for this experiment. The electric field in the bombarding region, including that due to space charge, should be as small as possible. The bombarding voltage should be kept near the threshold of 10.2 volts, (a) to reduce the spread of recoil angles and (b) to avoid background effects due to molecular hydrogen which enter at 11.5 volts. In practice, however, to obtain sufficient signal it is necessary to depart considerably from these principles.

The electron bombarder used consisted of a cathode, a control grid, an accelerator grid, and an anode as illustrated in Fig. 19. The cathode, G, was of the oxide-coated, indirectly heated type. The cathode and control grid, F, were completely enclosed by the accelerator grid electrode, E, which had grid wires only on the side facing the anode. This served to shield the interaction space, D, where excitation occurred, from the electric fields between the accelerator grid and the cathode. The shields B prevented radiation and evaporated matter from the hydrogen dissociator from reaching the electron bombarder and the detector. In the earlier models of this type of electron bombarder the anode C was absent, its purpose being served by the outer shell. With such an arrangement no metastable atoms were ever detected with certainty. This could have been ascribed to a lack of atomic hydrogen or to failure of the detection scheme. An independent proof of the presence of hydrogen atoms was made by allowing the hydrogen emerging from the dissociator to fall on a layer of yellow molybdenum oxide soot. The presence of hydrogen atoms was clearly indicated by the rapid reduction of the yellow oxide to the blue form. In the absence of a better check, the strong sensitivity of the detector to photons was taken as a fair indication that it would be sensitive to metastable hydrogen atoms as well. The electron bombarder was therefore indicated as a possible source of the difficulty. It was then established that the effects of space charge in the region between the accelerator grid and anode had been considerably underestimated. At the low electron energies used, 10 to 20 volts, the plate current of about 0.2 ma/cm^2 produced a large potential dip between the accelerator grid and the anode, which depended strongly on the distance separating the electrodes. The introduction of a separate anode reduced this clearance from 3 cm to about 1 cm or less. Thereafter, effects were immediately observed which were identified as being due to metastable hydrogen atoms.

It was found to be most advantageous to operate with an accelerator grid voltage of about 13.5 volts, and to bias the anode 3 volts positive with respect to the accelerator grid. The anode current was held at about 0.3 ma by adjusting the control grid voltage. These conditions were subject to considerable variation, the reasons for which will be discussed in Section 28. In general the operating conditions chosen represent a compromise between instability and signal strength.

The cathode base metal was nickel powder sintered to a molybdenum base and the coating was the usual triple mixture of barium, strontium, and calcium carbonates. The cathode area was approximately 1.5 cm^2. The control grid was formed of 0.002-in. diameter tungsten wires, 16 per in. and the accelerator grid of 0.002 in. diameter tungsten wires, 25 per in. The cathode-control grid and accelerator-control grid clearances were each about $\frac{1}{32}$ in. The accelerator grid-anode clearance was about $\frac{3}{8}$ in.

23. R-F and D.C. Quenching Fields

The metastable atoms are subjected to r-f or d.c. fields in the wave guide region J. The atoms enter and leave the region through the slits, I ($\frac{3}{16}$ in. wide by $\frac{5}{8}$ in. high). The wires, K, were installed long before any r-f fields were applied to aid in identifying the various electrons, ions, and photons that were at one time detected. Subsequently, they proved to be of great value in identifying metastable atoms, by virtue of the fact that an electric field applied between the wires will produce Stark effect mixing of the $2^2S_{1/2}$ and $2^2P_{1/2}$ states, thereby causing the metastable atoms to decay to the $1S$ state and cause a reduction in the electrometer current. In view of the difficulty encountered in maintaining a good supply of metastable atoms this feature of the apparatus was found to be indispensible, and not a temporary measure as originally intended. Furthermore, the transitions to the $2^2P_{1/2}$ levels occur at frequencies of 1500 to 6000 Mc/sec. at which the wave guide is beyond cut-off. For frequencies in that range the wires, K, were used as a two-wire transmission line.

The wires were positioned close to the line of edges of the slits, but without obscuring them. An electrostatic field produced by a voltage of 25 volts or more was sufficient to quench practically all of the metastable atoms. Since it is the electric field strength that determines the amount of quenching, the voltage required depends strongly on the configuration of the various electrodes and conductors.

Inasmuch as the r-f field configuration was rather complex and no attempt was made to terminate the line in a matched load, it would be difficult to estimate the r-f power required. It should naturally be in excess of the estimated value of Section 13. In practice, it was found that the signal generator used should deliver power in the neighborhood of 10 mw or more; the amount required depending on the frequency, presumably because of the frequency dependence of the load impedance.

Frequencies between 3000 and 10,000 Mc/sec. were obtained directly from $2K41$, $2K44$, or $2K39$ klystrons. Those frequencies near 12,000 Mc/sec. were obtained by doubling the frequency from a $2K44$ klystron in a $1N23$ crystal multiplier. Frequencies from 1500 to 2600 Mc/sec. were obtained from a $2C40$ lighthouse tube oscillator. The frequency stability resulting from

the use of ordinary regulated power supplies was found to be sufficient. The frequency, or rather the wavelength, of the radiation was measured by means of coaxial or cavity wave meters.

24. Magnetic Field

The magnetic field was produced by a small electromagnet used in this laboratory during the war for testing magnetrons. The pole pieces were 2 in. in diameter and tapered to 1 in. in diameter at the very ends. A 1-in. gap was used in this experiment. Magnetic fields of 3000 gauss or more were readily obtained. The magnet was supplied from a rectifier and filter, stabilized by a Sola constant voltage transformer.

The field was calibrated by moving the detector electrodes and inserting a small search coil into the center of the r-f region through the slit, I. The usual standard demagnetization procedure and magnetization curve method was followed in obtaining the calibration curve of magnetic field strength H *versus* magnet current, and throughout the measurements. The calibration was made to an accuracy of about 0.5 percent. This was more than sufficient accuracy, for it was found that the field in the r-f interaction space was non-uniform by some 33 gauss out of a total of 1000.

25. Gas Supply and Pumps

Hydrogen gas of commercial purity was used throughout. The Ohio Chemical Company claims that this gas is 99.7 percent, or better, of hydrogen, the balance being oxygen in the form of water vapor.

Gas was stored in a set of three one-liter glass bulbs and was admitted to the hydrogen dissociator through a fixed gas leak made by sealing an uncleaned piece of tungsten wire 0.020 in. diameter in a small bore Pyrex capillary tube. It was usually necessary to make three or four of these before obtaining one with the right degree of leakiness. The leak size was approximately 5×10^{-6} liter/sec. of air at one atmosphere. It was possible to control the rate of gas admission by adjusting the gas pressure in the storage bulbs below one atmosphere. The decay of the gas pressure in the storage bulbs during a run was undesirable, but its effect was small in comparison with fluctuations and changes due to other causes.

On account of the small size of the signals obtained, the gas admission rate was increased until the operating pressure in the apparatus was greater than 10^{-3} mm Hg. At somewhat higher pressures the diffusion pump would stop pumping. The pumping speed was evidently inadequate, but not so much so that the experiment could not be carried out.

The apparatus was evacuated through two one-inch pump leads (not shown in Fig. 19) by a three-stage fractionating pump. This was backed by a mechanical pump.

D. OBSERVATIONS

26. Size of the Signal

The detector current consisted of the signal, or current of electrons ejected by metastable atoms, and the background or current of photo-electrons arising primarily from excitation of molecular states in the background pressure of hydrogen molecules, and to some extent from excitation of atomic states other than the $2^2S_{1/2}$. At the electron energies used, the background was three or more times as large as the signal. A magnetic field of 100 gauss or more prevented the detection of ions and electrons from the electron bombarder.

The signal was observed as the galvanometer deflection obtained when a d.c. field large enough to quench practically all of the metastable atoms was applied to the wires K of Fig. 19 as described in Section 23. This deflection was usually some 20 to 50 cm and on occasion as much as 80 cm, or a current of 1.2×10^{-13} amp. This is smaller than the estimated value of Section 12 by a factor of about 40. An undetermined part of this discrepancy could be attributed to quenching by stray electric fields in the electron bombarder due to charges accumulated on insulating deposits on metal surfaces (Section 28). This has at times caused the signal to practically disappear. On the other hand, the maximum signal was obtained when the metal surfaces were cleared of all deposits. It seems unlikely that enough insulating material could remain to account for such a large amount of quenching.

In Eq. (20) all quantities but the detector efficiency have probably been underestimated so that S represents a lower bound of the expected signal. The discrepancy could be accounted for by taking η to be 1/80 instead of $\frac{1}{2}$ as in Section 12. A possible reason for such a low detection efficiency was indicated in Section 11.

27. Dependence of the Signal on the Magnetic Field

The observations covered a range of magnetic field intensity of about 50 to 3000 gauss. At each value of the magnetic field a portion of the beam of metastable atoms is lost by quenching due to the motional electric field given by Eq. (44). The amount of this loss increases with the magnetic field intensity, as can be seen from the discussions of Sections 6 and 16. It was observed that the signal decreased in general throughout the range covered and was fairly small at the highest fields, in qualitative agreement with the theory. The mode of construction of the apparatus did not permit an accurate study of this phenomenon. In addition to bad geometry, interfering effects in the electron gun would have made the results difficult to interpret.

28. Stability of the Signal

It was mentioned in Section 26 that the signal was subject to considerable variation. Part of this was ex-

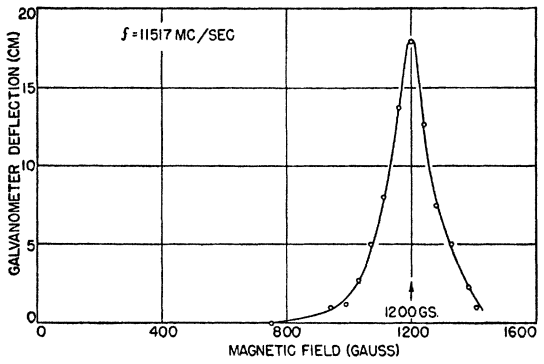

FIG. 21. Observed resonance curve.

plained in Section 27 as due to the magnetic field, but there was also an uncontrolled part principally caused by the electron bombarder. Some of this was due to the cathode which had to be replaced every three or four days because of emission poisoning. This was presumably caused by pump oil vapor or water vapor admitted with the hydrogen. As long as enough emission was available, the decay in the current could be corrected by adjustment of the control grid voltage.

In addition to emission poisoning, the optimum operating current and voltages of the electron bombarder kept changing as mentioned in Section 22. This was accompanied by a decrease in the signal which was appreciably less at the end of a run than at the beginning. The cause for this was not understood at the time, but is now known to be due to the formation of charged insulating layers on the grids and the anode. Thermal breakdown of pump oil vapor and perhaps wax is responsible for at least part of the material.‡ Dissociation under electron bombardment also occurs, and alkaline earth oxides evaporated from the cathode surface may also contribute. The charges accumulating on the layers add to the stray electric field quenching of the metastables, and thereby cause a decrease in the signal. They also have a large effect on the electronic behavior of the electron bombarder. This subject will be considered further in Part II.

In order to obtain a sufficiently large signal, it was necessary to increase the source pressure until the background pressure was just short of being sufficient to cause appreciable collision quenching. This condition was unfortunately accompanied by a large amount of short period fluctuation, largely in the background which, as indicated in Section 26, was already much larger than the signal. Fluctuations in the background were superposed on those in the beam of metastable atoms and placed a serious limitation on the accuracy of the measurements.

Changes in the detector efficiency could conceivably cause both long- and short-period variations; however, these have usually also been ascribable to other causes.

‡ Suggested to us by Dr. A. L. Samuel.

29. Procedure

It was shown in Section 14 that it would be very difficult to observe the shape of a resonance curve by holding the magnetic field fixed and varying the frequency. The reverse procedure was followed, wherein the oscillator frequency was held at a predetermined value and the magnetic field varied. The procedure was simply to demagnetize the magnet and to increase the magnetic field in steps, at each one observing the increase in the signal due to interruption of the power in the r-f line. Resonance curves obtained in this manner at various frequencies are plotted in Figs. 21 to 24. In these the galvanometer deflection obtained by interrupting the r-f power is plotted *versus* the magnetic field.

The variability of the electron bombarder, discussed in the previous section, made it necessary to seek a new optimum set of operating conditions before each run. This would usually suffice for two or three hours operation.

In view of the difficult experimental conditions, an excessive amount of r-f power was used throughout to enhance the size of the effect.

In principle, the effects of the long-period fluctuations and the variation of the signal with magnetic field could have been canceled by measuring the signal at each point by applying a d.c. quenching field, and expressing the r-f quenching as the ratio of r-f to d.c. quenching. This quantity when plotted *versus* H would have given more accurate resonance curves. On the whole, however, it was rather difficult to keep the apparatus in an operating condition long enough to take a resonance curve in the manner described above with only a few observations of the total signal. Thus it was not feasible to use the more accurate method. Nevertheless, the resonance curves were sufficiently sharp that they were not greatly in error due to variations of the signal with magnetic field strength.

E. ANALYSIS OF DATA AND RESULTS

30. Shape and Width of Resonance Curves

Some resonance curves typical of the better data are shown in Figs. 21 to 24 which represent examples of all

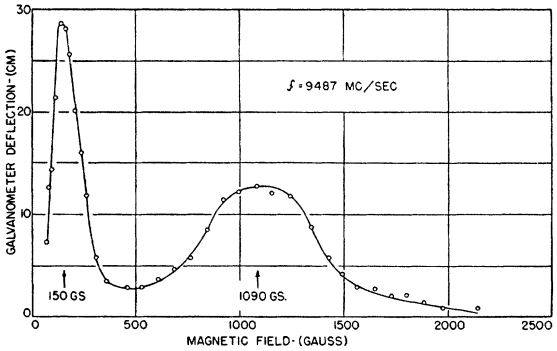

FIG. 22. Observed resonance curve.

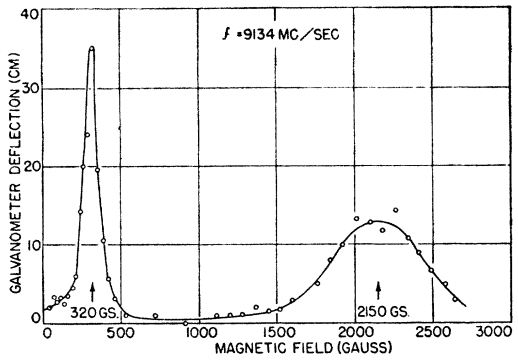

FIG. 23. Observed resonance curve.

observed transitions. It will be noted that these are just the transitions originating from the upper metastable level, α. In agreement with the considerations of Section 16, the other transitions were not observed.

Comparison of the resonance curves for hydrogen in Fig. 24, with the theoretical curves in Fig. 18(a) shows that the expected partially resolved hyperfine structure of the αf transition is completely obscured. Nor does the αe resonance exhibit the flat top shown in Fig. 18(b). Magnetic field inhomogeneity and r-f saturation could account for this discrepancy. The magnetic field inhomogeneity of 33 gauss per 1000 gauss in region J contributes to the smearing out of the hyperfine structure and adds to the expected theoretical width. As explained in Section 13, r-f saturation also adds to the half-width and thereby impairs the resolution of hyperfine structure. An additional cause of broadening may be due to the leakage of r-f through the rather large opening into the bombardment region. The atoms quenched there are in a magnetic field somewhat weaker than that found in the wave guide. Consequently, it would be expected that the half-widths of the peaks would considerably exceed the calculated values. This is shown in Table I. These calculated values take into account only the radiation width of 100 Mc/sec. and the unresolved hyperfine structure of the S and P levels. Doppler broadening may be neglected. The expected difference between hydrogen and deuterium is obscured, possibly because of greater saturation effects in the case of the latter.

31. Results

The resonance magnetic fields were located simply by taking the apparent peak in the case of sharp peaks, and by averaging the fields at half-amplitude for broad peaks. No corrections were made for overlap or other factors. The resonance magnetic fields so obtained at the various frequencies are plotted in Fig. 25. The theoretically calculated curves for the Zeeman effect, assuming validity of Dirac's theory, are plotted as solid lines, while for comparison with observed points, the calculated curves have been shifted down by 1000 Mc/sec. in the case of transitions to the $2^2P_{3/2}$ levels and up by 1000 Mc/sec. for those to the $2^2P_{1/2}$ levels. In view of the uncertainty introduced by inhomogeneity of the magnetic field and distortion of the peaks due to the falling off of the signal, no attempt was made to obtain a "best fit."

TABLE I. Half-widths of the peaks.

Substance	Transition	Obs. (Mc/sec.)	Calc. (Mc/sec.)
H	αf	410	219
H	αe	320	159
D	αf	400	128
D	αe	320	114

The results clearly indicate that contrary to the Dirac theory, but in essential agreement with Pasternack's hypothesis, the $2^2S_{1/2}$ level is higher than the $2^2P_{1/2}$ by about 1000 Mc/sec. (0.033 cm^{-1}) or about 9 percent of the spin relativity doublet separation. Within the precision of these results, there is no discrepancy between the Dirac theory and the doublet separation of the P levels.

The coincidence of the hydrogen and deuterium resonances indicates that with this precision, the $2^2S_{1/2}-2^2P_{1/2}$ shift for deuterium is the same as for hydrogen.

The authors have benefited greatly from the continuous cooperation and assistance of Dr. M. Phillips and Messrs. Bernstein, Costello, Dechert, and Richter, and other members of the Columbia Radiation Laboratory staff. The calculations referred to in Section 11 were made by Mr. D. Sternberg.

APPENDIX I. CONDITIONS IN A WOOD'S DISCHARGE

The absorption of radio waves by excited hydrogen atoms in a Wood's discharge tube depends on the populations of the various states. These in turn depend on the rates of production and decay of the excited atoms. It would involve a lengthy program of research to make quantitative calculations of these, and we shall be content here with the roughest sort of estimate. Only the $n=1$ and $n=2$ states of atomic hydrogen will be considered.

We shall assume that the $2p$ states decay to $1s$ at a rate corresponding to the natural lifetime $\tau_p=1.6\times10^{-9}$ sec., and that the excitation of $2p$ is due primarily to two causes: (1) electron bom-

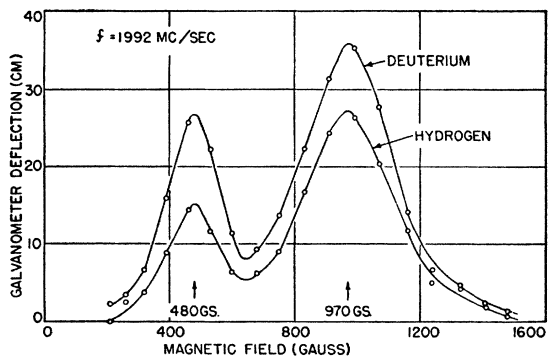

FIG. 24. Observed resonance curve showing similar curves obtained for hydrogen and deuterium.

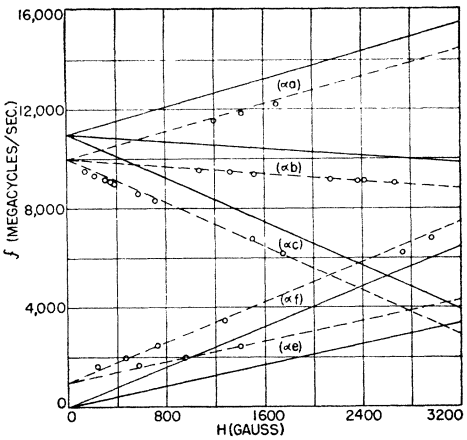

FIG. 25. Summary of data on resonance peaks. The solid curves correspond to the Dirac theory as in Fig. 13 while the dotted curves correspond to the modified curves of Fig. 15 with the $2^2S_{1/2}$ level raised by 1000 Mc/sec. The fit with the observed points clearly indicates the reality of such a shift.

bardment and (2) absorption of the Lyman resonance radiation emitted by other atoms. Since the absorption coefficient for this radiation is very large, a resonance radiation quantum can, on the average, only escape from the tube after a large number of absorptions and re-emissions. This number has been estimated[53] to be 500 to 1000 for typical discharge conditions. As a result, the effective decay rate of the $2p$ states is much smaller than that given by the natural lifetime, and the population of states $2p$ is correspondingly increased.

The situation is markedly different for the $2^2S_{1/2}$ state. As indicated in Section 9, excitation from $1^2S_{1/2}$ by electron bombardment is about one-tenth as likely as for $2p$ excitation. The imprisonment of resonance radiation plays no role here, for the $2^2S_{1/2}$ state cannot combine optically with the ground state. As a result, however, the $2^2S_{1/2}$ state under certain circumstances may be metastable, and despite the low rate of production, the population increased. As shown in Section 6, the decay rate of $2^2S_{1/2}$ increases with the electric field acting on the atom, and decreases with increasing separation of the states $2^2S_{1/2}$ and $2^2P_{1/2}$. If this separation is zero as given by the Dirac theory, the life of $2^2S_{1/2}$ in a typical Wood's discharge is a few times the natural life, but if the separation corresponds to 1000 Mc/sec., the life is increased to about 900 τ_p, and the population of $2^2S_{1/2}$ is correspondingly increased.

Let us consider the transitions between $2^2S_{1/2}$ and $2^2P_{3/2}$ induced by radio waves. If these states are populated in accordance with their statistical weights (equipartition), there will be no appreciable net absorption of r-f since the induced emission exactly cancels the induced absorption. (Spontaneous transitions between $2^2P_{3/2}$ and $2^2S_{1/2}$ occur at a negligible rate.) If the population of $2^2S_{1/2}$ is increased relative to $2^2P_{3/2}$, there will be a net absorption of r-f. If, on the other hand, $2^2P_{3/2}$ is more highly populated, there will be a net induced emission (negative absorption!).

On the basis of the preceding discussion alone, one would expect that the $2p$ levels would be about five to ten times more populated than the $2s$ levels. In that case, one would expect to find a negative absorption, and as estimated below, a large one. Admittedly the population estimates are rough. Still it would seem to require an accident for exact equipartition, unless there is some mechanism efficiently coupling $2^2S_{1/2}$ and $2^2P_{1/2}$. As indicated above, and as described quantitatively in Section 6, there is Stark effect coupling between these two states. If it were not for the entrappment of resonance radiation, the $2^2P_{1/2}$ state would not be sufficiently populated for the establishment of equipartition by this mechanism, but on the basis of the numerical estimates given above, and in Appendix II, it seems quite possible that it can occur, and that the absorption of r-f would be markedly reduced.

If equipartition is not achieved, a net absorption or induced emission can occur. In order to form an idea of the expected magnitude, we shall calculate the unbalanced rate of transitions induced by r-f from $2^2S_{1/2}$ to $2^2P_{3/2}$ ignoring the reverse transitions which might nearly cancel out or reverse the sign of the whole effect. Although the result may be an overestimate of the expected "absorption," it provides a convenient basis for discussion.

We proceed to estimate this absorption rate. In a typical Wood's discharge tube, there might be a pressure of 0.15 mm of mercury corresponding to a density of

$$n_{\mathrm{H}}=(0.15\times 2.687\times 10^{19})/(760)=5.3\times 10^{15} \tag{56}$$

hydrogen atoms per cubic centimeter. The number of atoms excited to $2^2S_{1/2}$ per unit volume per second is given by

$$J\sigma n_{\mathrm{H}}$$

where eJ is the electron current density, and σ is the excitation cross section. If we equate this to the assumed rate of density decay

$$n^*/(900\tau_p)$$

we obtain

$$n^*=900J\sigma\tau_p n_{\mathrm{H}}. \tag{57}$$

Taking an electron current density corresponding to 0.1 amp./cm^2

$$J=(0.1)/(1.602\times 10^{-19})=6.24\times 10^{17}\ \text{electron/cm}^2\text{/sec.}$$

and

$$\sigma=10^{-17}\ \text{cm}^2$$

(Section 9), we find

$$n^*=4.7\times 10^{10}\ \text{cm}^{-3} \tag{58}$$

in state $2^2S_{1/2}$.

We now consider the absorption of radio waves by these excited hydrogen atoms, taking as explained above, only the transitions to $2^2P_{3/2}$ into account. As in Section 13, the transition probability for absorption of radiation is

$$1/\tau_{\text{induced}}=(2\pi e^2S_0\gamma/c\hbar^2)\,|(|\hat{\mathbf{e}}\cdot\mathbf{r}|)|^2/[(\omega-\omega_0)^2+(\gamma/2)^2], \tag{59}$$

where S_0 is the incident energy flux density of the radiation having circular frequency ω and electric polarization vector parallel to the unit vector $\hat{\mathbf{e}}$, ω_0 is the circular resonance frequency, $(|\mathbf{r}|)$ is the matrix element of the coordinate vector $\mathbf{r}$ of the atomic electron for the transitions from $2^2S_{1/2}$ to $2^2P_{3/2}$, $\gamma=1/\tau_p$ is the reciprocal lifetime of the $2^2P_{3/2}$ state. For some estimates it is useful to use instead of a transition probability a cross section σ_{induced} for the absorption of a microwave photon. This is given by the equation

$$J_p\sigma_{\text{induced}}=1/\tau_{\text{induced}} \tag{60}$$

where J_p is the flux density of such photons. Now $J_p=S_0/\hbar\omega_0$ and hence

$$\sigma_{\text{induced}}=\hbar\omega_0/S_0\tau$$

or

$$\sigma_{\text{induced}}=2\pi(e^2/\hbar c)\,|(|\hat{\mathbf{e}}\cdot\mathbf{r}|)|^2\omega_0\gamma/[(\omega-\omega_0)^2+(\gamma/2)^2]. \tag{61}$$

For the sum of all transistions to the sub-levels of $2^2P_{3/2}$ one has $|(|\hat{\mathbf{e}}\cdot\mathbf{r}|)|^2$ equal to two-thirds of the value in which the sum is taken over all sub-levels of $2^2P_{1/2}$ and $2^2P_{3/2}$. This sum is just the value which would be calculated for the transitions from $2s$ to $2p$ ignoring electron spin. Hence[54]

$$|(|\hat{\mathbf{e}}\cdot\mathbf{r}|)|^2\rightarrow(\tfrac{2}{3})(27a_0^2/3)=6a_0^2. \tag{62}$$

At resonance

$$\omega=\omega_0=2\pi(10{,}950)\times 10^6\ \text{sec.}^{-1} \tag{63}$$

[53] Based on equations given by T. Holstein, Phys. Rev. **72**, 1212 (1947). See also L. M. Bieberman, J. Exp. Theor. Phys. **17**, 416 (1947).

[54] See reference 25, pp. 432 and 442.

and using

$$\gamma=1/(1.595\times10^{-9})=6.25\times10^{8}\text{ sec.}^{-1} \tag{64}$$

we find

$$\sigma_{\text{induced}}=3.4\times10^{-15}\text{ cm}^2. \tag{65}$$

For $n^*=4.7\times10^{10}$ atoms/cm^3 in state $2^2S_{1/2}$, the absorption coefficient would be $\mu=1.6\times10^{-4}$ cm^{-1}. This is a large absorption coefficient by modern microwave spectroscopic standards, but the breadth of the resonance $\gamma/2\pi\sim100$ Mc/sec. is many times the widths usually met in that field. As explained above, it is possible that this absorption is nearly all canceled out by the inverse transitions. In view, however, of the extreme crudeness of the numerical estimates, it is possible that some appreciable departure from equipartition may exist, and that an absorption or induced emission could be detected. It is therefore highly desirable that a search for such effects should be made, especially under discharge conditions which do not favor equipartition.

As a complicating factor, there will be a large and frequency dependent background absorption of microwaves in the discharge due to the electrons. Haase[18] found good agreement with an equation derived by Stewart[55]

$$\mu_{\text{electrons}}=(2e^2z\lambda^2N_e)/(\pi mc^3) \tag{66}$$

for the absorption coefficient of radiation with wave-length λ. Here z is the number of collisions with gas molecules per second experienced by an electron, and N_e is the number of free electrons per cubic centimeter. For the typical figures

$$\begin{gathered}z=0.95\times10^{9}\text{ sec.}^{-1}\\ N_e=2\times10^{9}\text{ cm}^{-3}\\ \lambda=3\text{ cm}\\ \mu_{\text{electrons}}=1.03\times10^{-4}\text{ cm}^{-1}.\end{gathered} \tag{67}$$

APPENDIX II. QUENCHING OF METASTABLE HYDROGEN ATOMS BY ELECTRIC FIELDS[56]

Our purpose here is to generalize the theory given by Bethe[25] for the effect of a uniform electric field on the lifetime of the $2^2S_{1/2}$ level, whose derivation did not take into account the removal of the degeneracy of $2^2S_{1/2}$ and $2^2P_{1/2}$.

We consider two excited levels with probability amplitudes a and b. The state a is metastable in the absence of an external electric field and has a small decay constant γ_a (double quantum emission to the ground state with life of $\frac{1}{7}$ sec.). Level b lies higher in energy by $E_b-E_a=\hbar\omega$ (ω may be negative), and decays to the ground state c with emission of resonance radiation at the rate $\gamma_b=1/\tau_p$. The equations of time dependent perturbation theory are then

$$\begin{aligned}i\hbar\dot a&=V^*e^{-i\omega t}b-\tfrac{1}{2}i\hbar\gamma_a a\\ i\hbar\dot b&=Ve^{i\omega t}a-\tfrac{1}{2}i\hbar\gamma_b b\end{aligned} \tag{68}$$

where $V=(b|e\mathbf{E}\cdot\mathbf{r}|a)$ is the matrix element of the perturbing electric field energy for the transition $a\rightarrow b$. The decay is treated phenomenologically by introduction of damping terms, but it is possible to justify this by writing out equations of the Wigner-Weisskopf[57] type.

The general solutions of Eqs. (68) are

$$\begin{aligned}a&=A_1\exp(\mu_1t)+A_2\exp(\mu_2t)\\ b&=-(\hbar/iV^*)[(\mu_1+\tfrac{1}{2}\gamma_a)A_1\exp((\mu_1+i\omega)t)\\ &\qquad+(\mu_2+\tfrac{1}{2}\gamma_a)A_2\exp((\mu_2+i\omega)t)]\end{aligned} \tag{69}$$

where μ_1 and μ_2 are the roots of the quadratic equation

$$(\mu+\tfrac{1}{2}\gamma_a)(\mu+i\omega+\tfrac{1}{2}\gamma_b)+|V|^2/\hbar^2=0. \tag{70}$$

In most applications, the γ_a-terms may be dropped. Then for small electric fields

$$\begin{aligned}\mu_1&\sim-i\omega-\tfrac{1}{2}\gamma_b\\ \mu_2&\sim-|V|^2/[\hbar^2(i\omega+\tfrac{1}{2}\gamma_b)].\end{aligned} \tag{71}$$

We represent the excitation of the metastable state by the initial conditions

$$a=1,\quad b=0\quad\text{at}\quad t=0. \tag{72}$$

This gives

$$\begin{aligned}A_1+A_2&=1\\ \mu_1A_1+\mu_2A_2&=0,\end{aligned} \tag{73}$$

whence

$$A_1=\mu_2/(\mu_2-\mu_1),\quad A_2=-\mu_1/(\mu_2-\mu_1). \tag{74}$$

The probability that level a is occupied after passage of time t is

$$|a|^2=|A_1\exp(\mu_1t)+A_2\exp(\mu_2t)|^2. \tag{75}$$

The first term has a small coefficient and is strongly damped. Since $|A_2|\sim1$, the effective decay rate is

$$\gamma_{\text{Stark}}=\mu_2+\mu_2^*=\gamma_b|V|^2/[\hbar^2(\omega^2+\tfrac{1}{4}\gamma^2)]. \tag{76}$$

For $\omega=0$, this reduces to Bethe's result. In case there are several well separated levels, b, none of which is too strongly coupled to a, the decay rates are simply additive.

In the limit $|V|^2\rightarrow0$, the exact solutions give $\mu_2+\mu_2^*=\gamma_a$ while for $|V|^2/\hbar^2[\omega^2+\frac{1}{4}\gamma_b^2]\rightarrow\infty$,

$$\mu_i+\mu_i^*=\gamma_b/2$$

for $i=1$, 2, giving the expected results. The approximate expression (76) suffices for most purposes.

In the discussion of Appendix I, a problem arose concerning the mechanism whereby equipartition could be established between the $2^2P_{1/2}$ and $2^2S_{1/2}$ states. Without any such mechanism, it was estimated that the population of $2^2P_{1/2}$ might be as much as 12 times that of $2^2S_{1/2}$. Consider now an atom excited by resonance radiation to $2^2P_{1/2}$. It decays rapidly to $1^2S_{1/2}$ by reemission of resonance radiation, but because of the Stark coupling, there is a small probability that a transition to the long lived $2^2S_{1/2}$ state take place. This probability may be calculated by solving Eqs. (68) subject to the initial conditions

$$b=1,\quad a=0\quad\text{at}\quad t=0. \tag{77}$$

The terms in μ_1 are rapidly damped, and the probability for reaching the metastable state is

$$\begin{aligned}|a|^2=|A_2'|^2&=|\mu_2/(\mu_2-\mu_1)|^2\simeq|V|^2/\hbar^2[\omega^2+\tfrac{1}{4}\gamma_b^2]\\ &=(\gamma_{\text{Stark}}/\gamma_b)\sim1/800.\end{aligned} \tag{78}$$

Since the resonance radiation on the average requires 400 to 1000 absorptions and re-emissions before escaping, there is a high probability that a long-lived $2^2S_{1/2}$ state will be populated before the escape can occur. Consequently there would seem to be at least one plausible mechanism for establishment of equipartition between $2^2P_{1/2}$ and $2^2S_{1/2}$.

APPENDIX III. DISTRIBUTION IN RECOIL ANGLES

As indicated in Section 10, the hydrogen atoms which are excited to the metastable state experience a recoil measured by an angle Θ giving the change in their direction of motion. Our task here is to compute the distribution in recoil angles. Let M be the mass of the atom, $\mathbf{V}_0$ its initial velocity, $\mathbf{V}_1$ its final velocity, and let the velocity of the bombarding electron of mass m be $\mathbf{v}_0$, that of the outgoing electron be $\mathbf{v}_1$. The momentum balance for the collision is then

$$M\mathbf{V}_0+m\mathbf{v}_0=M\mathbf{V}_1+m\mathbf{v}_1. \tag{79}$$

The energy balance is approximately

$$\tfrac{1}{2}mv_0^2-\tfrac{1}{2}mv_1^2=(\tfrac{3}{4})hcR \tag{80}$$

neglecting the kinetic energy change for the atom.

The momentum conservation may be represented as shown in Fig. 26 where ϵ is the angle of the inelastically scattered electron.

[55] J. Q. Stewart, Phys. Rev. **22**, 324 (1923).

[56] P. Caldirola, Nuovo Cimento **5**, 399 (1948) considered the effect of the level shift on the Stark quenching of $2^2S_{1/2}$, but his calculation is subject to the error made in reference 26 mentioned in Section 6.

[57] See, for example, G. Wentzel, *Handbuch der Physik* (1933), second edition, Vol. 24/1, p. 752.

The circle is intended to represent the spherical locus of the vector $m\mathbf{v}_1$ and it must be remembered that $\mathbf{V}_1$ may therefore lie out of the plane of $\mathbf{V}_0$ and $\mathbf{v}_0$. For definite values of V_0 and v_0 the angle Θ will have a range of values because of the distribution in ϵ. To simplify matters, we shall assume this distribution to be spherically symmetrical. This assumption should not be too bad near the threshold where v_1 is relatively small and the outgoing wave function is mostly one of zero orbital angular momentum.

From an experimental standpoint, we are interested in horizontal and vertical recoil angles ψ and χ separately. We may approximately set

$$\tan\psi=(mv_0-mv_1')/(MV_0) \tag{81}$$

where v_1' is the magnitude of the projection of $\mathbf{v}_1$ along $\mathbf{v}_0$. Likewise

$$\tan\chi=(mv_1'')/(MV_0), \tag{82}$$

where v_1'' is the magnitude of the projection of $\mathbf{v}_1$ perpendicular to the horizontal plane. Since the angles ψ and χ are fairly small, the tangents may be replaced by the angles in radians. Under the assumption of a spherical distribution in $\mathbf{v}_1$, the probability distribution in v_1' is uniform between the limits v_1 and $-v_1$ and likewise[58] for v_1''. Hence the probability distribution in ψ is uniform for $\psi_1\leqslant\psi\leqslant\psi_2$ where

$$\psi_1=(mv_0-mv_1)/(MV_0) \quad \text{and} \quad \psi_2=(mv_0+mv_1)/(MV_0) \tag{83}$$

and it may be written as

$$P(V_0;\psi)d\psi=\begin{cases}(MV_0/2mv_1)d\psi & \psi_1\leqslant\psi\leqslant\psi_2\\ 0 & \text{otherwise}\end{cases} \tag{84}$$

satisfying the normalization condition

$$\int_{\psi_1}^{\psi_2}P(V_0;\psi)d\psi=1. \tag{85}$$

Likewise

$$P(V_0;\chi)d\chi=\begin{cases}(MV_0/2mv_1)d\chi & -\chi_1\leqslant\chi\leqslant+\chi_1\\ 0 & \text{otherwise}\end{cases} \tag{86}$$

where

$$\chi_1=mv_1/MV_0. \tag{87}$$

Expressions (84) and (86) are valid for definite initial velocities $\mathbf{v}_0$ and $\mathbf{V}_0$ of bombarding electrons and hydrogen atoms. The bombarding electrons may be assumed to be monoenergetic. The distribution of velocities of the atoms will give rise to an additional spread of recoil angles. Assuming thermal equilibrium in the oven at temperature T, the probability distribution of velocities in the beam is given by

$$N(V_0)dV_0=AV_0^3\exp(-V_0^2/U^2) \tag{88}$$

[58] The correlation of ψ and χ is neglected.

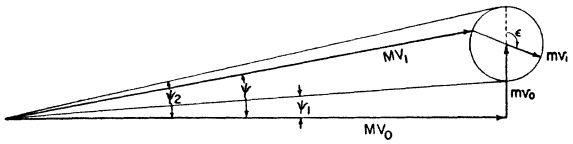

FIG. 26. Diagram showing momentum and energy relations for the recoil deflection experienced by a hydrogen atom excited to the $2^2S_{1/2}$ state by electron bombardment at 13.6 ev.

where A is determined from the normalization condition to be $A=2U^{-4}$, and the parameter U from $\frac{1}{2}mU^2=kT$. The most probable velocity contained in the beam is given by $(3/2)^{\frac{1}{2}}U$.

The combined distribution in ψ is given by

$$P(\psi)=\int_0^\infty N(V_0)P(V_0;\psi)dV_0=(M/2mv_1)\int_{V_a}^{V_b}N(V_0)V_0dV_0 \tag{89}$$

where

$$V_a=(mv_0-mv_1)/(M\psi) \quad \text{and} \quad V_b=(mv_0+mv_1)/(M\psi). \tag{90}$$

With the substitution $y=V_0/U$ this becomes

$$P(\psi)=(MU/mv_1)\int_{y_1}^{y_2}y^4\exp(-y^2)dy, \tag{91}$$

where

$$y_1=V_a/U \quad \text{and} \quad y_2=V_b/U. \tag{92}$$

Likewise

$$P(\chi)=(MU/mv_1)\int_0^{y_3}y^4\exp(-y^2)dy, \tag{93}$$

where

$$y_3=(mv_1/M\chi). \tag{94}$$

Bombardment at the Threshold

These expressions considerably simplify at the threshold where $v_1\to 0$. There is no vertical recoil and the horizontal distribution reduces to

$$P(\psi)=2(mv_0/MU)^4\psi^{-5}\exp[-(mv_0/MU\psi)^2]. \tag{95}$$

This is plotted in Fig. 7 for an oven temperature of $T=2600°\text{K}$ where $U=6.55\times10^5$ cm/sec. and $(3/2)^{\frac{1}{2}}U=8.03\times10^5$ cm/sec. gives the most probable atom velocity.

Bombardment at 13.6 e.v.

At this energy, $v_0=\alpha c$ and

$$v_1=\tfrac{1}{2}v_0=\tfrac{1}{2}\alpha c,$$

where α is the fine structure constant, so that

$$y_1=\tfrac{1}{3}y_2=(m\alpha c/2MU\psi), \quad y_3=(m\alpha c/2MU\chi).$$

The integrals (91) and (93) were calculated numerically and plots of $P(\psi)$ and $P(\chi)$ are shown in Fig. 7.